Theses and Dissertations

1973

Simulation of grass in the hydraulic laboratory

Chhun V. Heang
Lehigh University

Follow this and additional works at: https://preserve.lehigh.edu/etd

Part of the Civil Engineering Commons

Recommended Citation

SIMULATION OF GRASS
IN THE HYDRAULIC LABORATORY

by
Chhun V. Heang
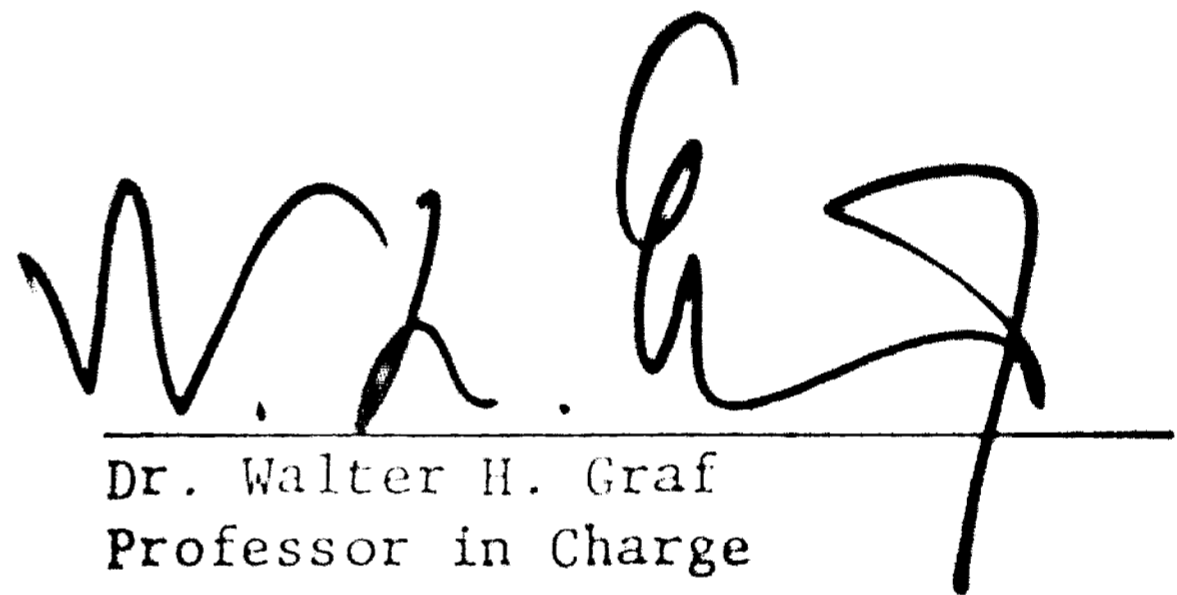
A Thesis
Presented to the Graduate Committee
of Lehigh University
in Candidacy for the Degree of
Master of Science
in
Civil Engineering
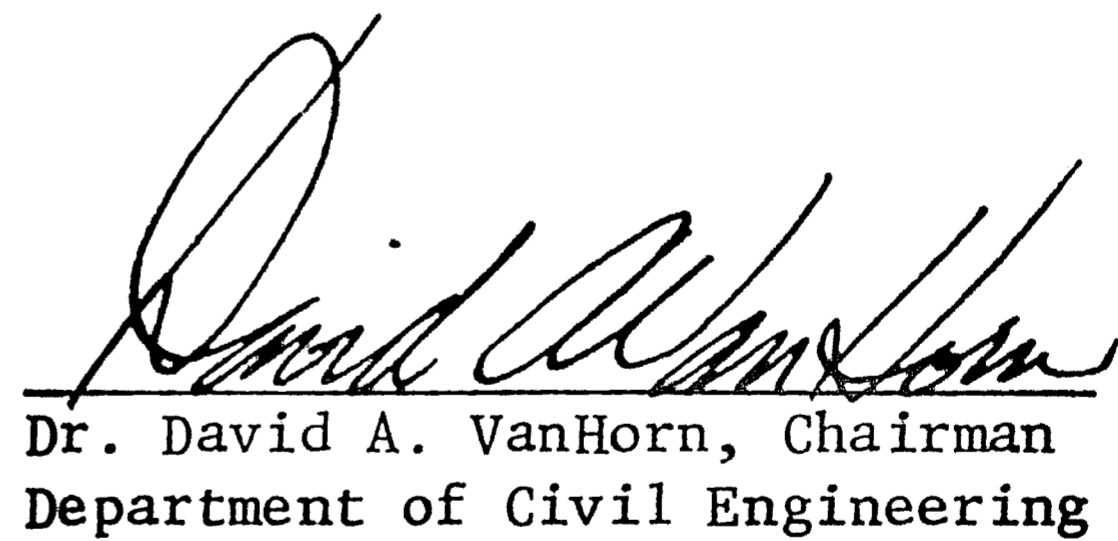
Lehigh University
1973

CERTIFICATE OF APPROVAL

This thesis is accepted and approved in partial fulfillment of the requirements for the degree of Master of Science.

Date: 29-June-1972

Dr. Walter H. Graf
Professor in Charge

Dr. David A. VanHorn, Chairman
Department of Civil Engineering

ACKNOWLEDGMENTS

TABLE OF CONTENTS

TABLE OF CONTENTS (Contd.)

LIST OF RECURRING SYMBOLS

A	entire cross-sectional area; in square feet
A_B	cross-sectional area with respect to the flume bottom in Fig. 4.2; in square feet
A_w	cross-sectional area pertaining to both sides of the walls in Fig. 4.2; in square feet
B, B'	widths of the channels in Figs. 3.2, 3.3, and 3.4; in feet
D	measured depth at each station in Figs. 3.3 and 3.4; in feet
$\bar{D}$	average cross-sectional depth; in feet
D_u	uniform flow depth; in feet
N_R	flow-Reynolds number; $N_R = (4 R_h \bar{u})/\nu$
$n_{A \cdot 1}, n_{A \cdot 2}$	roughness coefficient for Astroturf No. 1 and Astroturf No. 2
n_B	roughness coefficient of the bottom
n_w	roughness coefficient of the side wall
n_{wood}	roughness coefficient of the wooden surface
P	wetted perimeter of the entire cross section; in feet
Q	flow discharge, in cubic feet per second
R_B	hydraulic radius pertaining to the flume bottom; in feet
R_h	hydraulic radius pertaining to the entire cross section; in feet
R_w	hydraulic radius pertaining to the side walls; in feet
S_o	longitudinal slope of the channels
$\bar{u}$	average velocity of the flow; in feet per second
α, α'	angles of the side slopes, shown in Figs. 3.3 and 3.4
ΔH	manometer deflection; in feet

LIST OF FIGURES

LIST OF FIGURES (Contd.)

LIST OF TABLES

ABSTRACT

The present study is concerned with the experimental investigation of artificial grass, known as Astroturf. Two types of Astroturf were investigated. Astroturf consists of a thick mattress which simulates the soil surface where groups of grass are fixed in equidistant longitudinal and radial rows. Each group of grass possesses strips which simulate the grass blades that radiate both upward and outward from the mattress.

The experiments were conducted in one rectangular flume and two triangular flumes located in the Hydraulic Laboratory of Lehigh University. Investigated in the rectangular flume were two types of Astroturf and a wooden surface. The latter was used only to compare the results. Investigated in the triangular flumes was only Astroturf No. 1.

The discharge, Q, the hydraulic radius, R_h, the wetted perimeter, P, and the slope, S_o, were measured. With this information and the use of Manning's equation, the n-values were calculated. The computed roughness coefficients were plotted against both the uniform-flow depths and the Reynolds numbers. The plots showed a dependency of the n-value on the flow depth and/or the Reynolds number. However, this dependency disappeared at high discharge. The n-values selected from this study were those which were independent of the flow discharge and/or flow depth. They were taken as

$$n_{A \cdot 1} = 0.0326 \text{ for Astroturf No. 1,}$$

$$n_{A \cdot 2} = 0.0275 \text{ for Astroturf No. 2, and}$$

$$n_{wood} = 0.0150 \text{ for the wooden surface.}$$

These n-values are in good agreement with the experimental results for "real" grass found in the hydraulic literature. It is concluded, therefore, that Astroturf will be a useful material when simulating grassed channels in the hydraulic laboratory.

1. INTRODUCTION

1.1 Presence of Grass in Channels

The presence of grass in channels is the source of considerable flow turbulence, which results in noticeable loss in energy and flow retardance. The flow retardance refers to water held back by the surface roughness. This back water effect may be responsible for flooding and thus might become a menace to civilization in the flood plains. Although such instances could be termed disadvantages, the presence of grass in channels can be an advantage as well. Earth channels are built to carry water; frequently these earth channels are subject to soil erosion. PARSONS (1963) reported that grass lining in channels may protect both the streambed and streambank from being eroded in many ways. Namely, it will remarkably reduce the average velocity of the flow and the shear stress at the soil surface to a value below that required to cause erosion. REE (1949) prepared a comparative diagram shown in Fig. 1.1. It can be seen from this diagram that the water
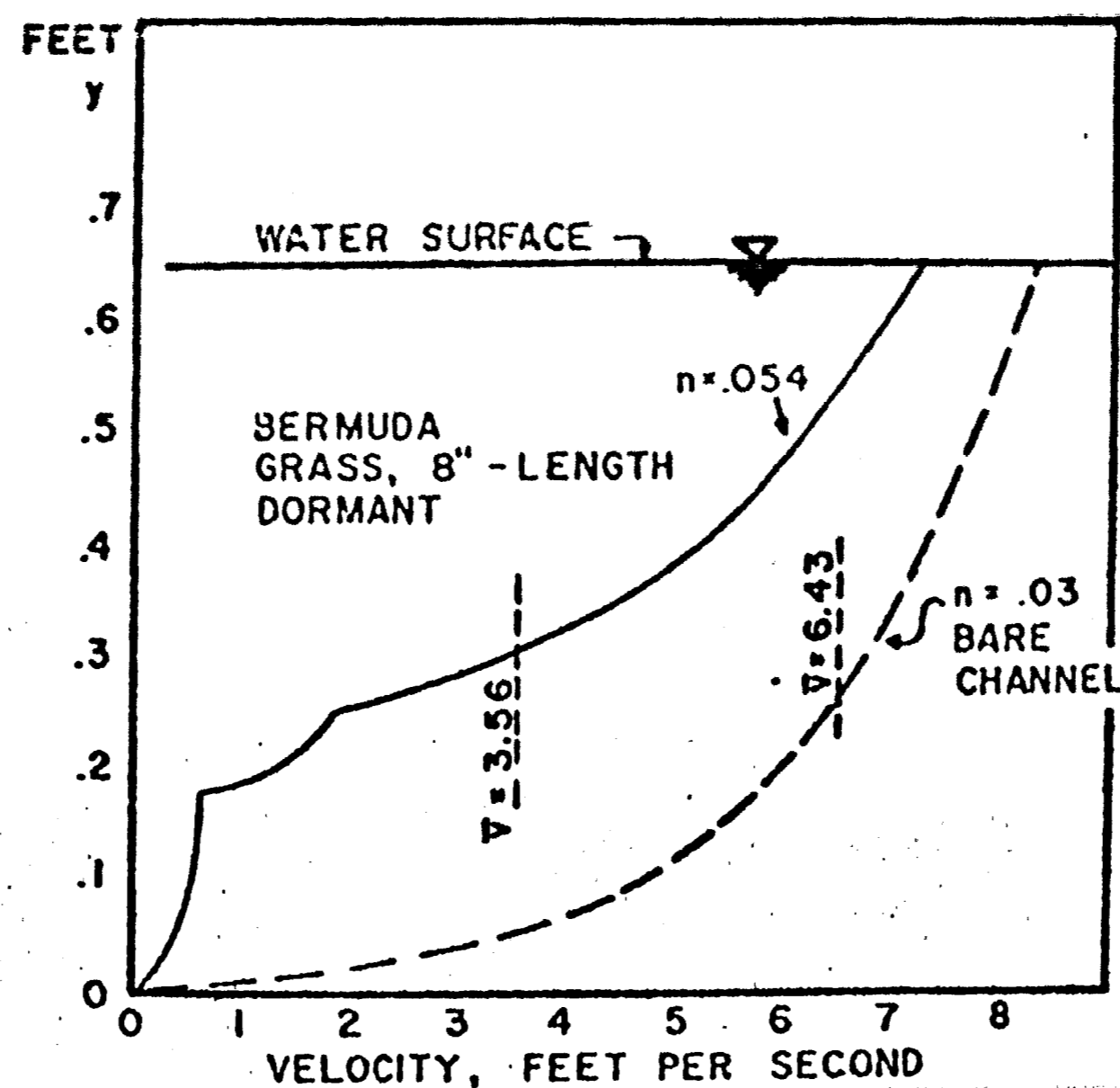
Fig. 1.1: Flow Over Grass (after REE (1949))

-3-

velocity - and the shear stress as well - is drastically reduced with the grass lining. Another advantage is that grass lining may result in inducing deposition of sediments and thus will contribute to bed and bank stability. Whether or not grass channels present advantages or disadvantages to the flow dynamics or to the environment, the hydraulics of the channels has to be investigated. It is an important task of hydraulics to study the flow-roughness coefficient of grassed surfaces.

1.2 Manning's Relation

The fundamental empirical equation used in the flow computation was developed by Manning (1889) for either a canal or a river. In English units the equation reads

$$\bar{u} = \frac{1.486}{n} R_h^{2/3} S_o^{1/2} \tag{1.1}$$

where $\bar{u}$ is the average velocity of the flow, R_h is the hydraulic radius which approximates the depth of the flow in a case of a wide, one-dimensional flow channel, S_o is the energy slope of the steady uniform flow, which can be replaced by the water-surface slope without introducing any serious error, and n is the so-called Manning roughness coefficient. Equation (1.1) was derived for the turbulent flow, which requires that the Reynolds number be greater than 2,000. For the computation of flow in cross sections with composite roughness, a method was developed by HORTON (1933) and EINSTEIN (1942).

From the available literature the Manning roughness coefficients for various types of vegetation were collected by CHOW

(1959, pp. 110-113). Table 1.1 summarizes this information on the roughness coefficients for grass.

Type of Channels and Description	Minimum	Normal	Maximum
1/ Lined or Built-Up Channels - Vegetal Lining	0.030	—	0.500
2/ Excavated or Dredge Channels - Short grass, few weeds - Grass, some weeds	0.022 0.025	0.027 0.030	0.033 0.033
3/ Flood Plains - Short grass - High grass	0.025 0.030	0.030 0.035	0.035 0.050

Table 1.1: Values of Roughness Coefficients, n, for Grass
(after CHOW (1959, pp. 110-113))

REE et al. (1949) have conducted experiments for the U. S. Soil Conservation Service on a series of channels lined with various types of natural grass. They found that for a given type of grass and for a given channel, the roughness coefficient will not remain the same under all conditions. It was found that the n-value depended on the stage and discharge of the flow. Figure 1.2 illustrates the variation of the n-value with mean stage or depth for three different rivers. It can be noticed that in general the roughness coefficient increases as the discharge and/or the stage decreases. This is due to the fact that at low depths the materials (sand, bedform, grass, etc.) of the rivers are relatively more exposed to the flow than at high depths. On the other hand, the roughness coefficient can be higher at high
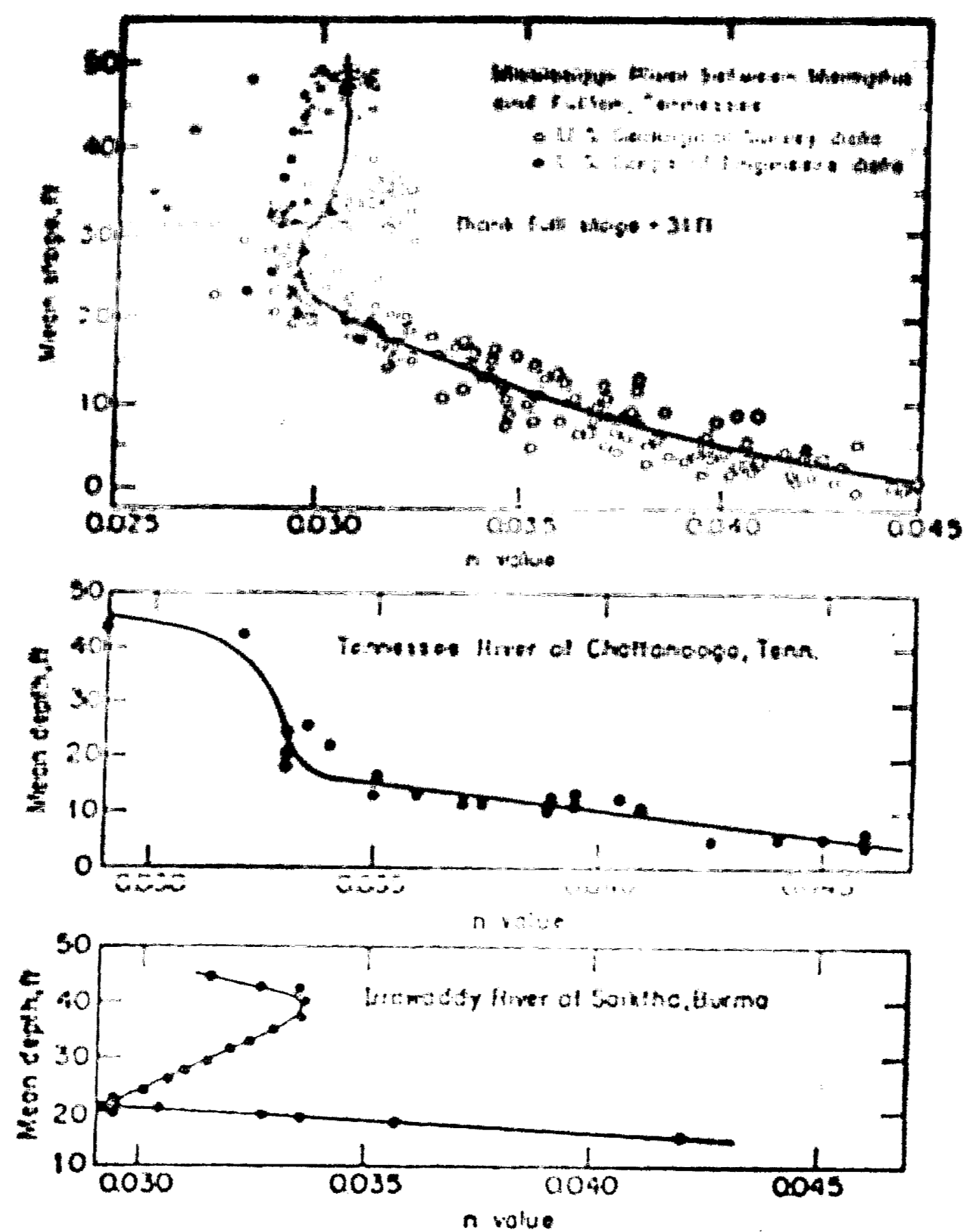
Fig. 1.2: Variation of n-Value with Stage and Discharge (after CHOW (1959, p. 105))

discharge and/or high depth. This fact would be **observed when water** overflows the huge flood plains of the river.

1.3 Scope of the Present Study

Numerous times, it becomes **necessary to investigate grass-** lined canals or rivers in the hydraulic laboratory. The inevitable question arises as to how the roughness coefficient of grass can be modeled. The present investigation studies the possibility of using artificial "grass". Artificial grass is now available on the market under the name of Astroturf. Two types of Astroturf are studied herein.

2. EXPERIMENTAL EQUIPMENT

2.1 Experimental Set-Up for Rectangular Channel

The experiments were conducted in a glass-walled open channel located in the Hydraulics Laboratory of Lehigh University. Figure 2.1 shows the entire testing equipment. The experimental set-up was arranged in loop form. As can be seen from Fig. 2.1, a centrifugal pump was responsible for pumping water from an underground water tank (or sump) to a constant head tank, which in turn released its water through the supply line. The water passed through a Venturi meter and then reached the stilling basin upstream from the glass-walled flume. Leaving the stilling basin the water passed into the glass-walled flume in which the desired slopes were adjusted.

2.1.1 Pump and Motor

Water was circulated by a centrifugal pump having a capacity of 1850 gpm under a head of 70 ft [21.3 m] while operating at 1750 rpm. Figure 2.2 shows two pumps, of which pump No. 1 was used. This pump was driven by a 40 hp electric motor. The revolutions per second of the motor shaft, as well as those of the pump itself, could be changed by manipulating a rheostat.

2.1.2 Head Tank

A constant head tank from which the water flowed by gravity through 8-inch [203-mm] pipes was equipped with an overflow device to maintain a constant water elevation in the head tank. This can be seen in Fig. 2.1.
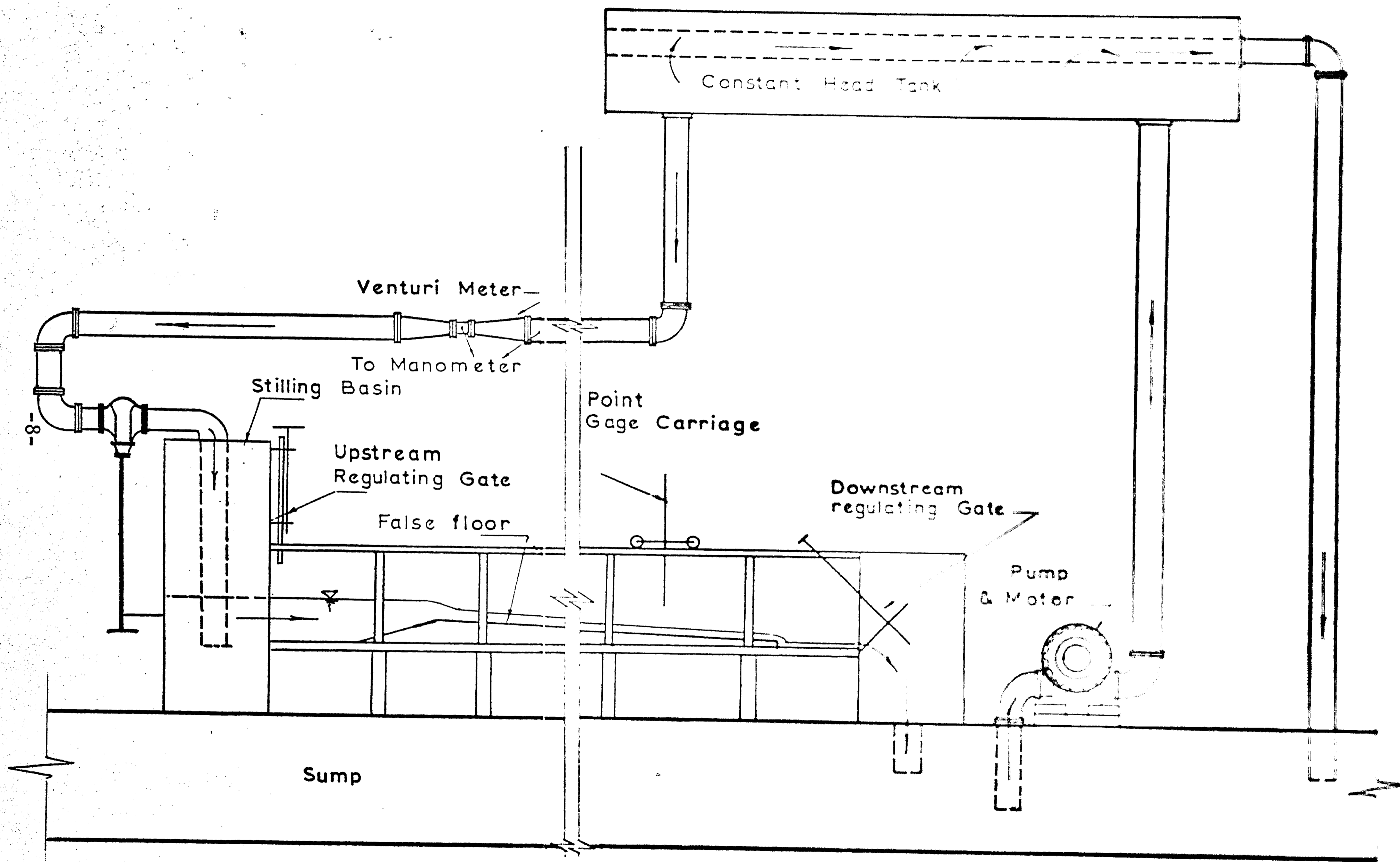
Fig. 2.1: Arrangement of the Glass-Walled Flume (Not to Scale)

2.1.3 Venturi Meter

The flow rate through the channel was measured by a Venturi meter which was installed in the supply line. The Venturi meter, shown in Fig. 2.1, was 4 ft [1.22 m] long and had a throat diameter of 5 in [127 mm]. The unit had been calibrated by previous experiments, and the following rating equation was obtained:

$$Q = 1.05 \, \Delta H^{0.522} \tag{2.1}$$

where Q is the discharge rate in cfs and ΔH is the difference of heads in feet of water, read from the manometer.

2.1.4 Stilling Basin

The stilling basin, as can be seen in Fig. 2.1, was located upstream from the glass-walled flume. The stilling baffles were built into this basin to damp the water surface oscillation.

2.1.5 Flume

The glass-walled flume was a rectangular open channel. The flume was 24 ft [7.32 m] long and 1.5 ft [0.45 m] wide. It was equipped with a tail gate. Figure 2.3 shows the flume (looking downstream) with the point gage mounted on a carriage. The false bottom, to be seen in Fig. 2.4, was 16 ft [4.87 m] long and made of two pieces of plywood. Eight adjusting screws were used. Each of these was attached at 4-foot [1.22 m] intervals along both sides of the support structure to make the slope adjusting possible.

Fig. 2.2:   Pumps, Motors, and Rheostats

Fig. 2.3:   Glass-Wall Flume
            (Looking Downstream)

Glass-Walled Flume

Point Gauge Carriage

A—A

False Floor

Support Structure

Slope Adjusting Screws

Sealing
(Tape)

To Sump

LAB. FLOOR

Details of the Slope

1 False Floor (Plywood)
2 Support Structure (Wood)
3 Slope Adjusting Screws
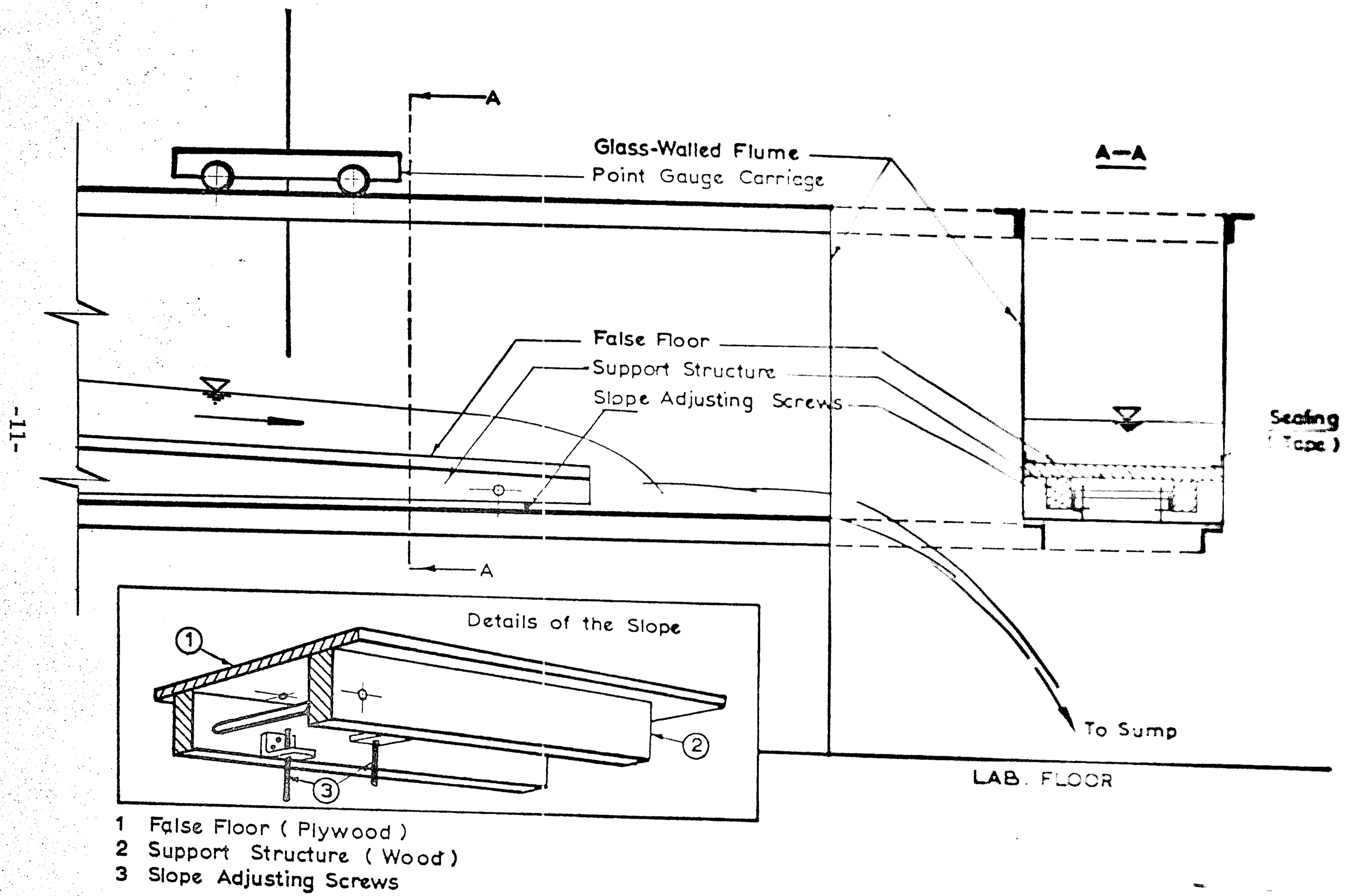
Fig. 2.4: Downstream End of the Test Section (Not to Scale)

2.1.6 Point Gage

Figure 2.5 shows the point gage used in the investigation. It was equipped with vernier scale which enabled measurements to an accuracy of 0.001 ft [3.05×10^{-4} m]. The point gage was made to have three degrees of freedom; that is, it could move, with respect to the flume, longitudinally, transversally, and vertically.
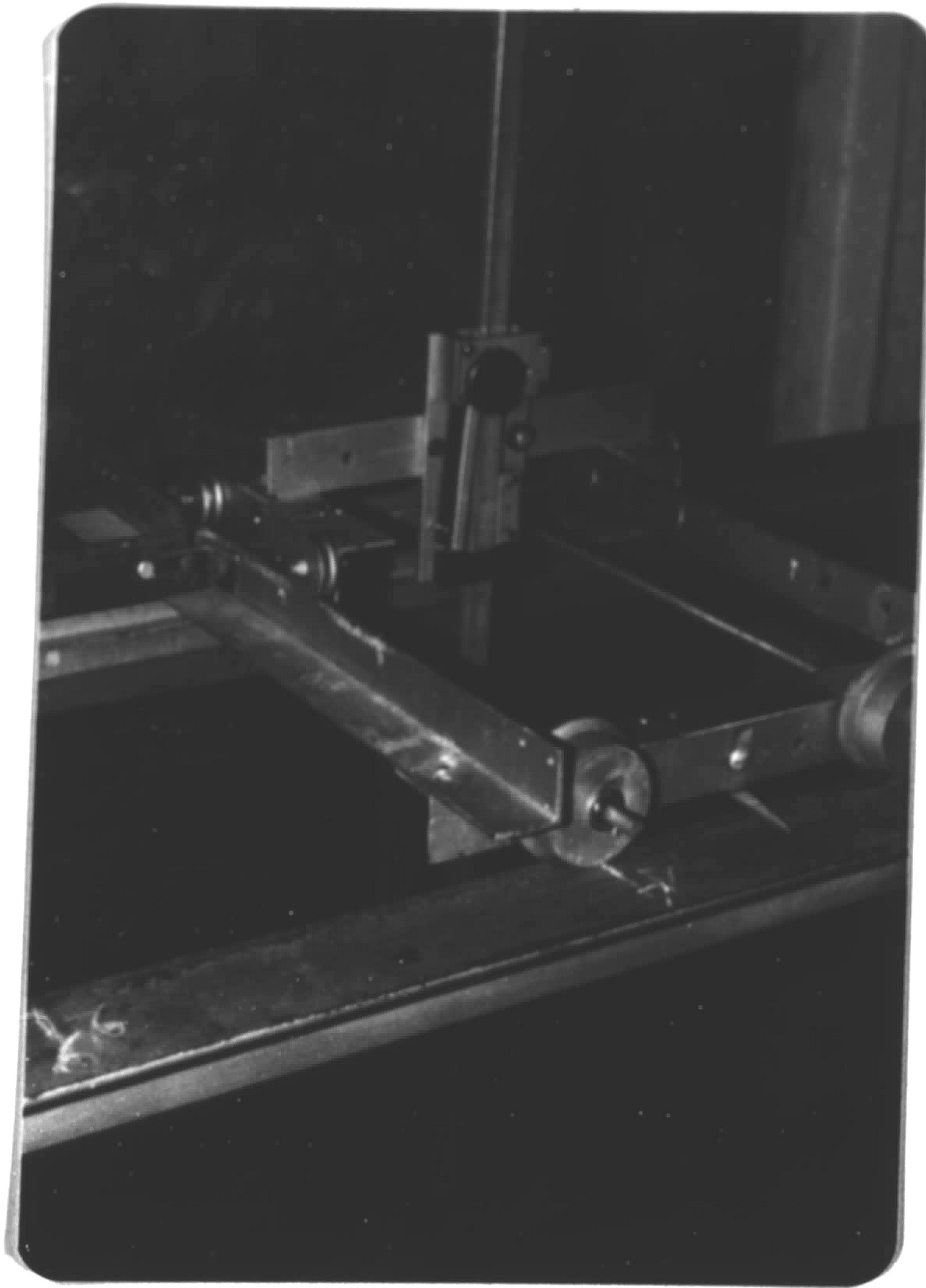
Fig. 2.5: Point Gage Mounted on a Carriage

2.2 Experimental Set-Up for Triangular Channel

In order to obtain higher discharges another experimental set-up was used. Figure 2.6 shows the schematic diagram of the testing arrangement. Two pumps (B) raised water from the sump (A) into the pressure tank (D). From there the water flowed into the head tank (N) and then through the channel (J). Subsequently, the water returned to the main sump (A).

2.2.1 Pumps and Motors

Figure 2.6 shows two pumps, each of which was driven by a 9B type HF Induction Motor equipped with a rheostat. Motor No. 1 had a rating of 40 hp with a maximal speed of 1740 rpm. Motor No. 2 had a rating of 35 hp with a maximal speed of 1720 rpm. Each pump was a single-stage, double-suction, centrifugal pump.

2.2.2 Pressure Tank and Supply Line

The circular pressure tank (D) was 5 1/2 ft [1.68 m] in diameter and 34 ft [10.4 m] high. Water leaving the pressure tank was controlled by the supply valve (E). The rate of discharge allowed to be delivered to the manifold discharge pipe (M) was measured by means of a 4-inch [101-mm] orifice meter (H).

2.2.3 Manometers

The 4-inch [101-mm] orifice (H) in a 12-inch [305-mm] supply pipe was placed upstream from the supply valve (E). It was either an air-water manometer (F) for lower discharges (Q ≤ 0.5 cfs) or a liquid-water manometer (G) for higher discharges (Q > 0.5 cfs). The specific

LEGEND

A	Sump		**H**	Orifice
B	Pump		**J**	Channel
C	Valve		**M**	Manifold
D	Pressure Tank			Discharge Pipe
E	Supply Valve		**N**	Head Tank
F	Air-Water Manometer			
G	Liquid-Water Manometer			
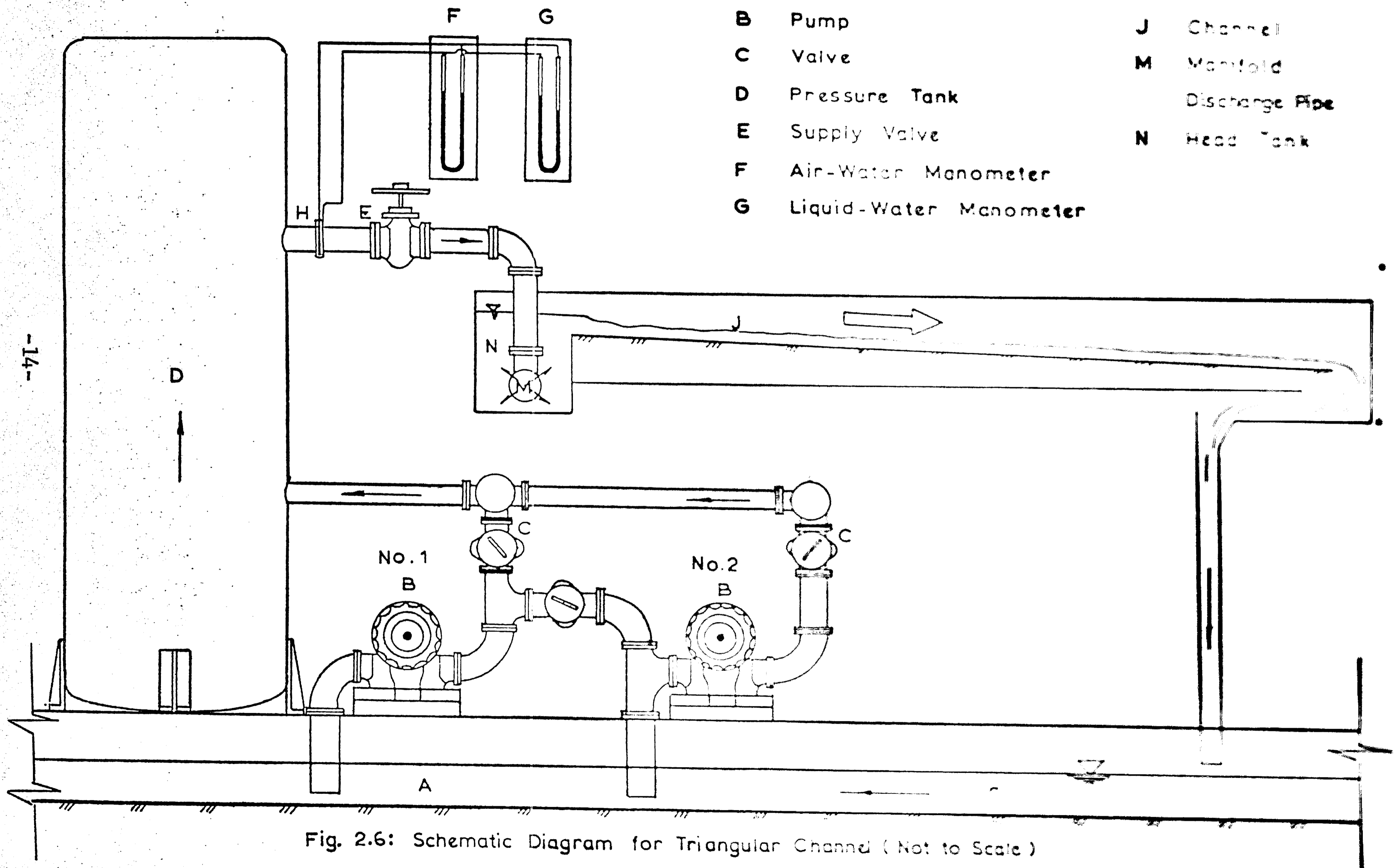
Fig. 2.6: Schematic Diagram for Triangular Channel (Not to Scale)

gravity of the manometer liquid was 2.95. The unit had been calibrated, and the volumetric expression was given by

$$Q = 0.42 \cdot \Delta H^{0.5} \tag{2.2}$$

where Q is the flow rate of water in cfs and ΔH is the pressure head difference in feet of water [x 0.3048 m].

2.2.4 Channel

The testing channel, which is shown with Fig. 2.7, was 28 ft [8.54 m] long and 16 ft [4.89 m] wide. Figure 2.8 shows both the plan view and the elevation view of the model construction. Two steel frames supported the swale slope (O) and the back slope (P) which form a triangular channel. Both swale slope and back slope were made of 3/4-inch [19-mm] plywood upon which Astroturf No. 1 was stapled. These slopes were joined together by means of hinges which were welded to the invert of the channel to prevent the two steel frames from being separated and to provide freedom for the frames to rotate about the invert whenever the swale and back slopes were desired.

A main beam W8 x 40I supported the entire length of the invert. The mid-point deflection of this beam was eliminated by providing support at mid-span. The longitudinal slope could reach its maximal value of 8.00%. The side slopes could be adjusted by means of four 3/4-inch [19-mm] threaded tension rods (Q). The longitudinal wall (V) could be removed whenever the flow over both side slopes was needed.
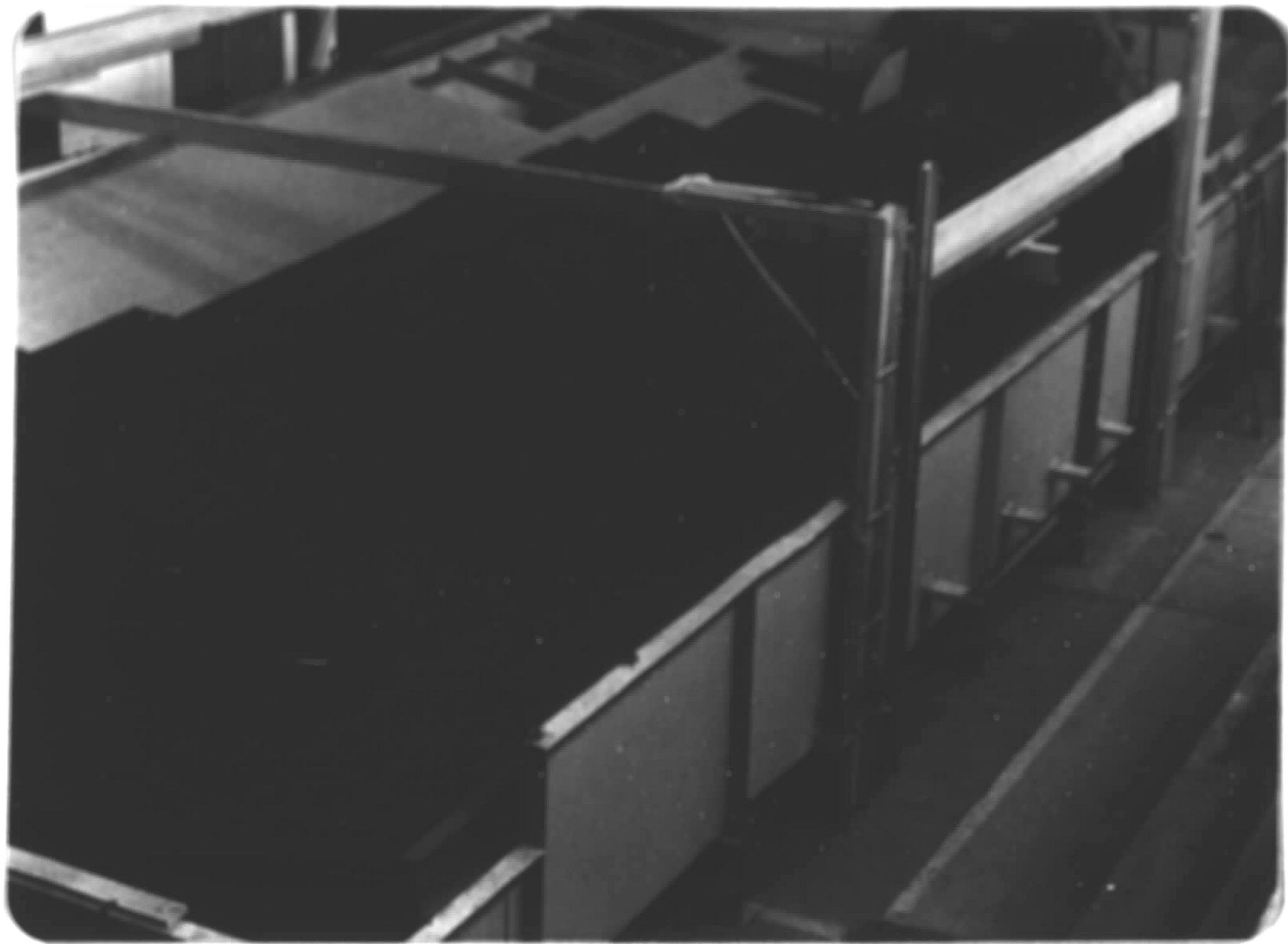
Fig. 2.7:   Triangular Flume with Astroturf No. 1
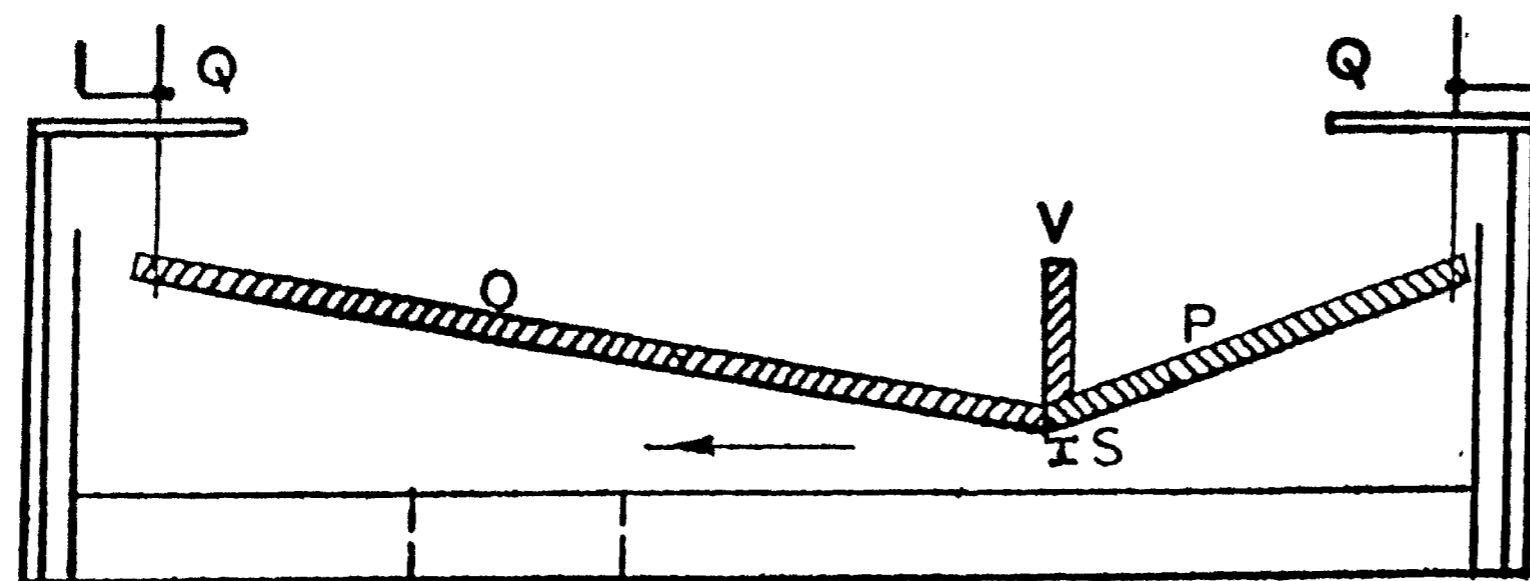
LEGEND

H Orifice

M Manifold Discharge Pipe

N Head Tank

O Swale Slope

P Back Slope

Q Side-Slope Adjusting Rods

S Main Supporting I-Beam

U Opening to Sump

V Removable Wall

(a) Plan View

(b) Elevation View

Fig. 2.8: Plan and Elevation View
of the Channel (Not to Scale)

-17-

2.2.5 Point Gage

In all depth measurements a point gage graduated to 0.001 ft [3.05 · 10⁻⁵ m] was used. The gage was mounted on a carriage that rolled along a 3-inch [76.3-mm] by 5-inch [127-mm] aluminum rectangular track which was 17 ft [5.18 m] long. The rectangular track was placed 2 ft [0.6 m] above the invert and was at right angles to the invert of the channel. To permit the beam to travel freely above the invert, both ends of the aluminum member were supported by a monorail system.

2.3 Artificial Roughnesses

There were three roughnesses investigated in this study. Two of them, Astroturf No. 1 and Astroturf No. 2, were the artificial grasses, products of Monsanto Chemical Company. The third roughness was simply the wood surface of the false bottom.

Figure 2.9 shows Astroturf No. 1 consisting of a 1/16-inch [1.6-mm] thick mattress which simulates the soil surface where groups of grass are fixed in equidistant longitudinal and radial rows of 2/5 inch [10 mm]. Each group of grass possesses eight strips forming a compact base of 1/4 inch [6.34 mm] in diameter. At the very top, that is to say, at a distance 15/16 inch [23.8 mm] from the mattress, the simulating blades radiate outward so that the surface of the Astroturf resembles that of the natural grass.

Astroturf No. 2, as can be seen in Fig. 2.10, is smaller in size than Astroturf No. 1. Also it consists of groups of strips. Each group is 1/36 inch [0.7 mm] in diameter at the base and contains
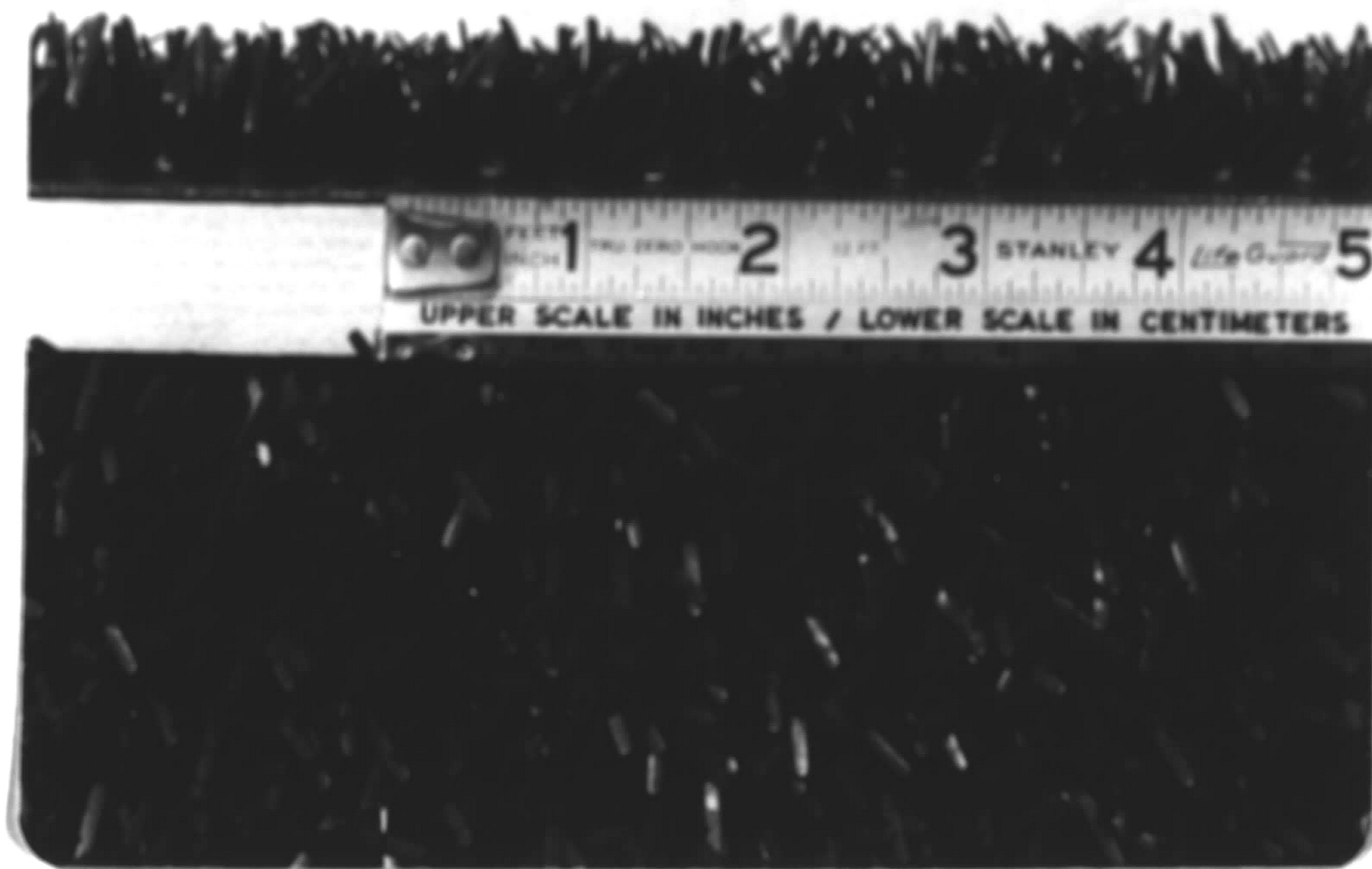
Fig. 2.9: Astroturf No. 1

Fig. 2.10: Astroturf No. 2

16 strips that rise upward and radiate outward. The mattress on which
the groups are mounted equidistant in rows is 1/16 inch [1.6 mm] thick.
The rows, shown in Fig. 2.11, form with both transversal and longi-
tudinal edge of the mattress an angle of 45°. The distance between
each group in any row is 1/8 inch [3.2 mm] and the distance between
adjacent rows is also 1/8 inch [3.2 mm]. The height, H_a, of Astroturf
No. 2 is 2.5/8 inch [7.95 mm]. Each blade is 0.093 in [1 mm] wide.
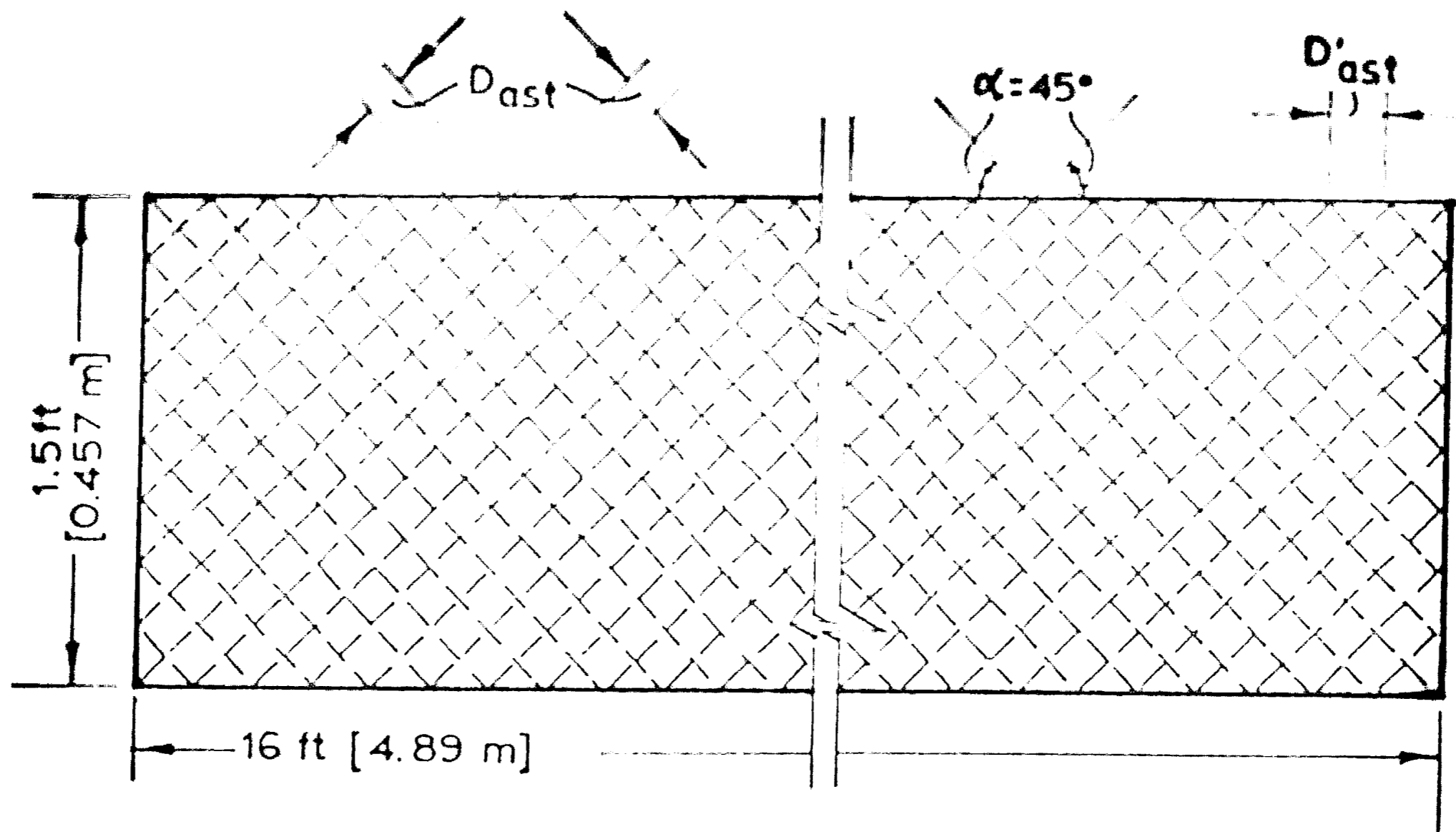
Fig. 2.11: Strip (16.0'x 1.5' [4.89 m X 0.457 m])
Disposition of Astroturf No.2
(Not to Scale)

Table 2.1 is the summary of size of both astroturfs. The
symbols can be seen in Fig. 2.12.
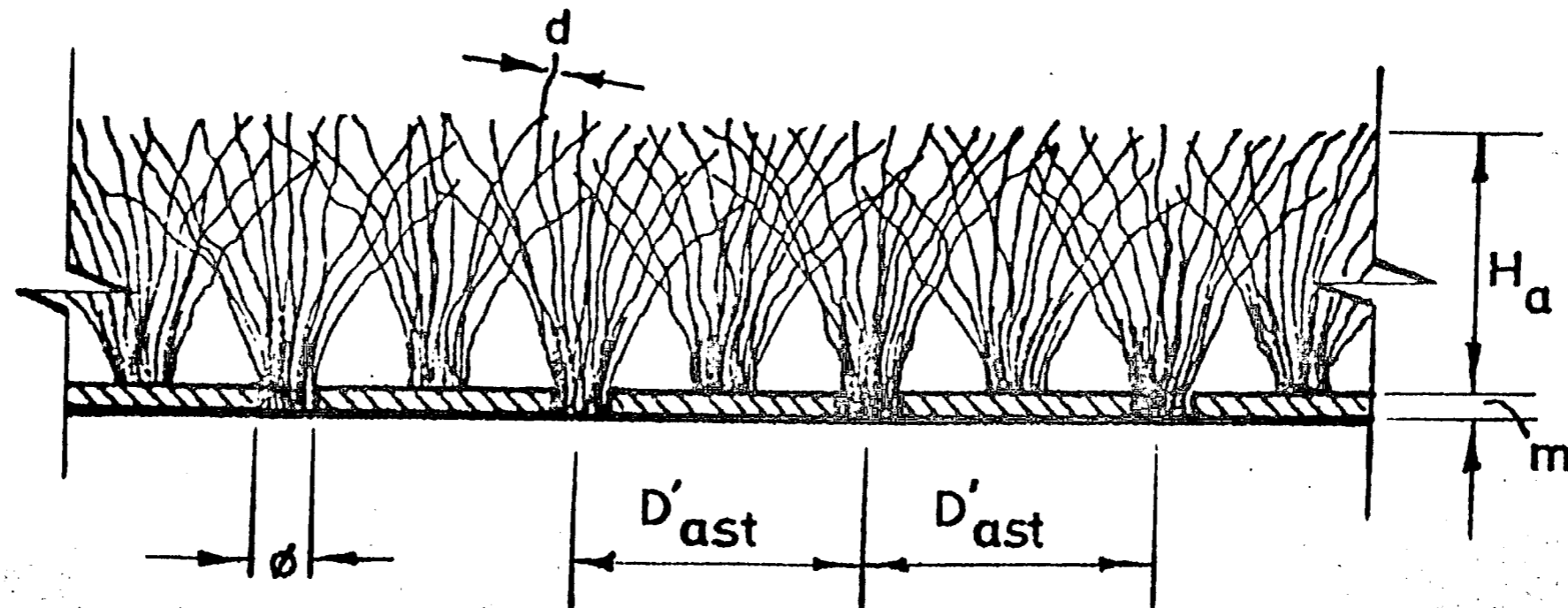
Fig. 2.12: Schematic Sketch of Astroturf
(Not to Scale)

-20-

A_{st}	m		Ø		n_a	d		H_a		S		D_{ast}		D'_{ast}	
	in	[mm]	in	[mm]	- -	in	[mm]	in	[mm]	in	[mm]	in	[mm]	in	[mm]
1	2		3		4	5		6							
No. 1	1/16	[1.6]	1/4	[6.35]	8	11/135	[2]	15/16	[23.]						3.7
No. 2	1/16	[1.6]	1/36	[0.7]	16	11/270	[1]	2.5/8							[5]

Table 2.1: Summary of Size of Both Astroturfs[*]

[*]See the following for explanation of symbols column by column in Table 2.1:

(1) A_{st} (type of astroturf)

(2) m   (thickness of the mattress)

(3) Ø   (diameter of each group at base)

(4) n_a (total number of strips or blades in each group)

(5) d   (width of blade)

(6) H_a (height of groups as well as that of astroturf)

(7) S   (distance between axes of groups in any row)

(8) D_{ast} (distance between adjacent rows)

(9) D'_{ast} (distance between adjacent transversal rows)

3. EXPERIMENTAL PROCEDURE

3.1 Rectangular Flume

Slope Setting: Each slope, S_o - shown in Tables A-1, A-2, and A-3 of Appendix A -, was set (α) by changing the slope of the false floor, shown in Figs. 2.3 and 2.4, with the 8 (4 on each side) slope adjusting screws and (β) by using a level (transit).

After the slope was adjusted, 2-inch [50.8-mm] self-sticking transparent tape and permagum were used to seal the joints where the longitudinal plywood edges and the glass-walled surfaces met in order to make the space below the slope waterproof. Since it was impossible to keep the slope as it had been adjusted, it was necessary to verify the slope frequently.

Grass Stapling: Astroturf No. 1 was investigated first. It was cut to fit the width of the flume and was brought into the flume to cover the slope. Figure 3.1 shows Astroturf No. 1, which was made ready to be stapled to the slope that had been adjusted.

To prevent the astroturf from being washed away down the slope at high discharges, the mattresses of both sizes of astroturf were stapled to the wooden slope at a density of one staple per 30 square inches.

Discharge Measurements: For each opening of the valve located upstream from the stilling basin, the water was allowed
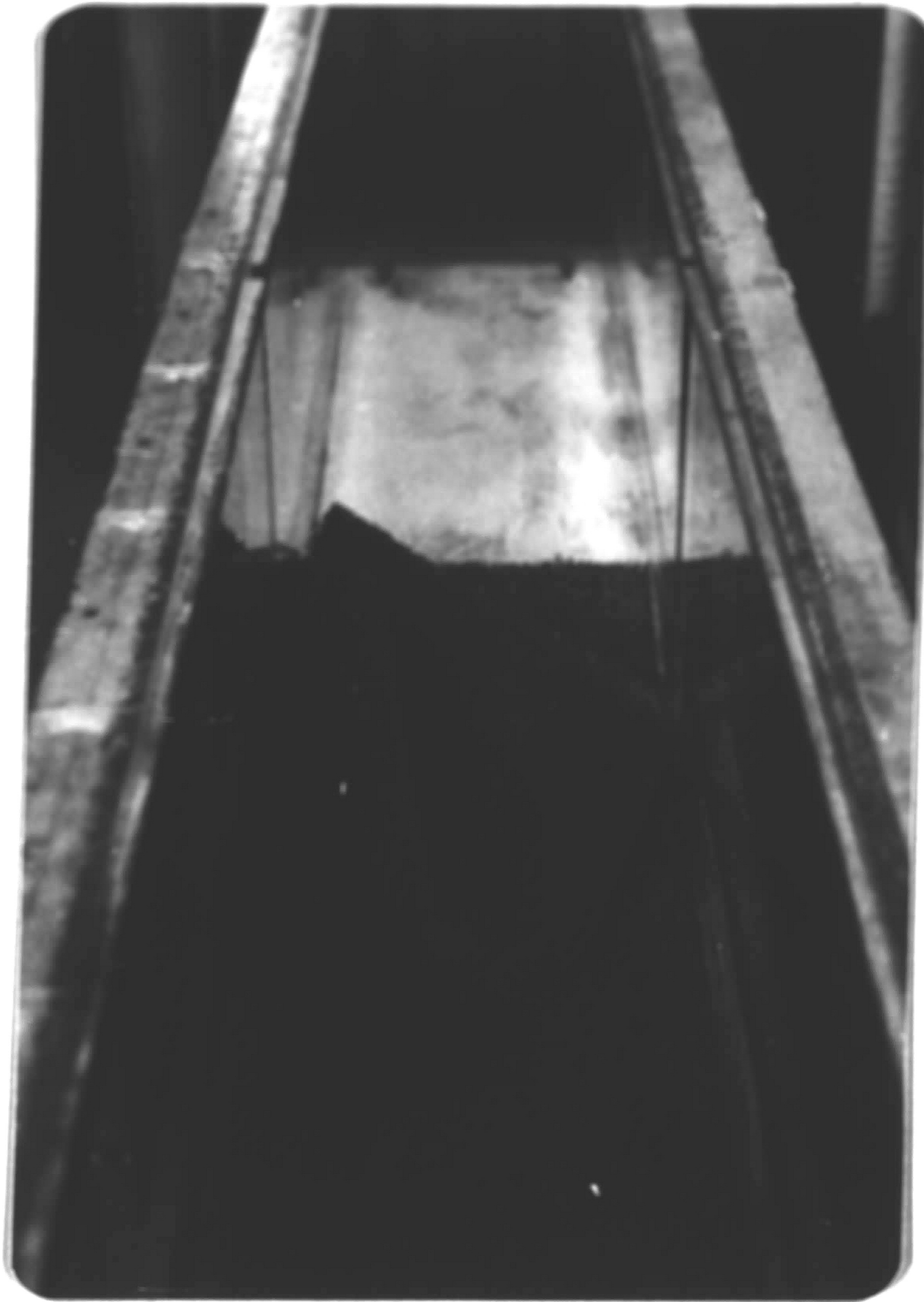
Fig. 3.1: Astroturf No. 1 Ready to be Stapled

for five minutes to flow through the flume in order to stabilize the

flow rate. Then the air-water manometer was read off to obtain the

manometer deflection, ΔH, which was used with Eq. (2.1) to compute

the flow rate.

Depth Measurements: For each slope ten different discharges

were studied. Each discharge could be controlled by the opening of the

supply valve located immediately upstream from the stilling basin, as

can be seen in Fig. 2.1.

Depth measurements were made at cross sections located at every foot along the channel's test section, which was 16 ft [4.89 m] long. The depth at each cross section was known as the average of the three depths measured at the quarter points of the cross section, as shown in Fig. 3.2. At each point the difference between the water level
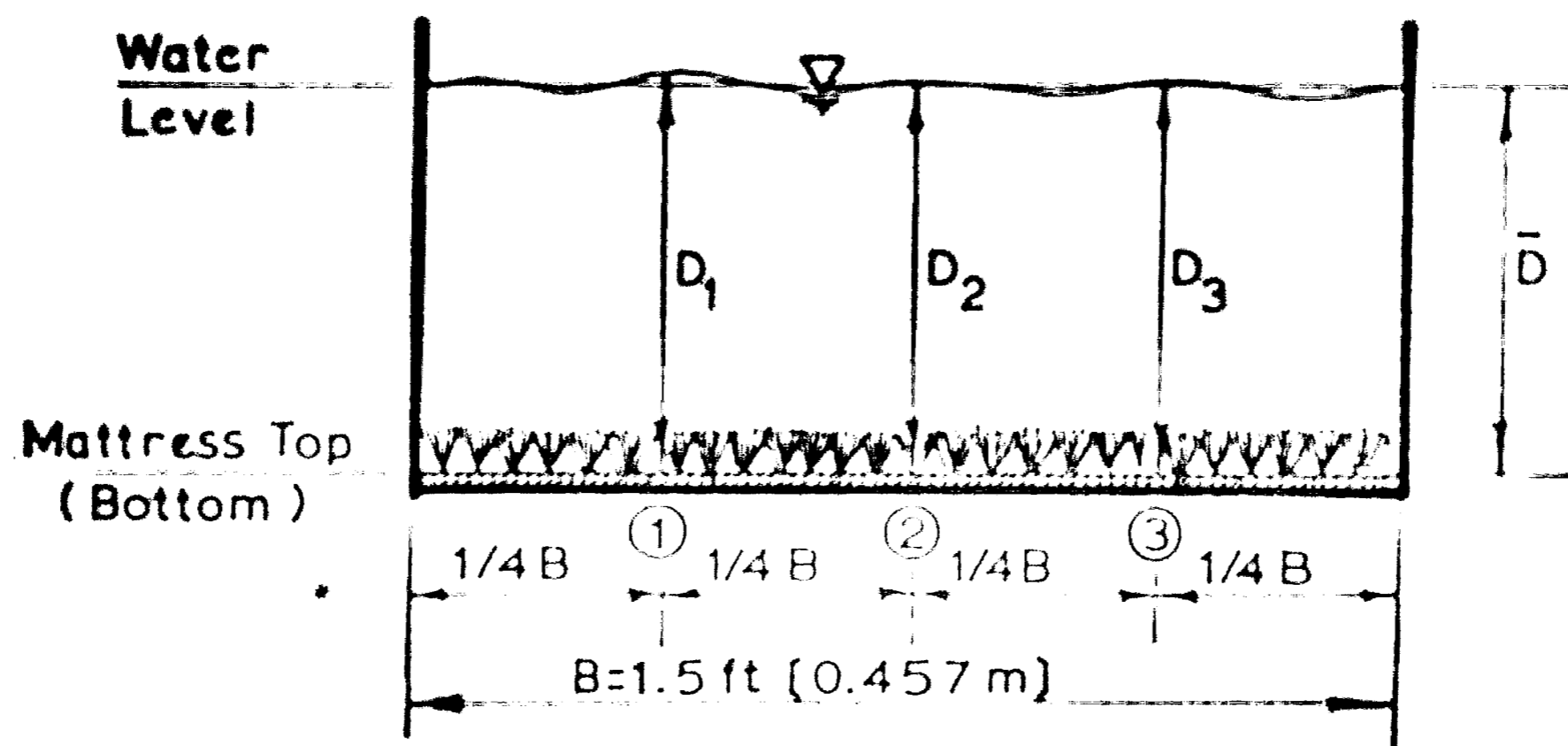
Fig. 3.2: Depth Measurements

reading and the bottom reading (the point gage was lowered to the mattress) was taken as the depth, D_i. (The subscript, i, refers to the quarter point number.) Now that the depths, D_1, D_2, and D_3, were known, the average depth, $\overline{D}$, for the cross section would be obtained as follows:

$$\overline{D} = \frac{D_1 + D_2 + D_3}{3} \tag{3.1}$$

The same procedure was used for all cross sections along the test section; that is, from station 0 to station 16.

Width of the Channel: The width of the rectangular flume is constant, (B = 1.5 ft [0.457 m]).

-24-

The whole procedure was repeated for Astroturf No. 2 and for
the wood, whose data and results are shown in Tables A-2 and A-3 of
Appendix A, respectively.

3.2 Triangular Flume

Grass Stapling: Astroturf No. 1 was brought into the flume
and was stapled to the wooden side slopes and to the longitudinal wall.

Slope Setting: Four longitudinal slopes were used; see
Tables A-4 and A-5 of Appendix A. They were adjusted in the same way
as described before for the rectangular flume. However, a crank instead
of adjusting screws was used to lift the longitudinal slope up and down.
One side slope was constant at $S = 1/6$; the other side slope was either
at $S' = 1/4$ or at the vertical position. (See Figs. 3.3 and 3.4.)

Discharge Measurements: As can be seen from Tables A-4 and
A-5 in Appendix A, ten different discharges were also investigated for
each slope setting. The reader is referred to the discharge measure-
ments for the rectangular flume because the procedure was the same.
The discharge itself was computed according to Eq. (2.2).

Depth Measurements: Depth measurements were made within a
5 ft [1.52 m] - long reach located in the middle part of the 28 ft
[8.54 m] - long test section. This reach was reasonably uniform,
being as far as possible removed from the flow transition zones.
Figures 3.3 and 3.4 show that the depth, D, can be measured directly
by the point gage or it can be computed in terms of the angles,
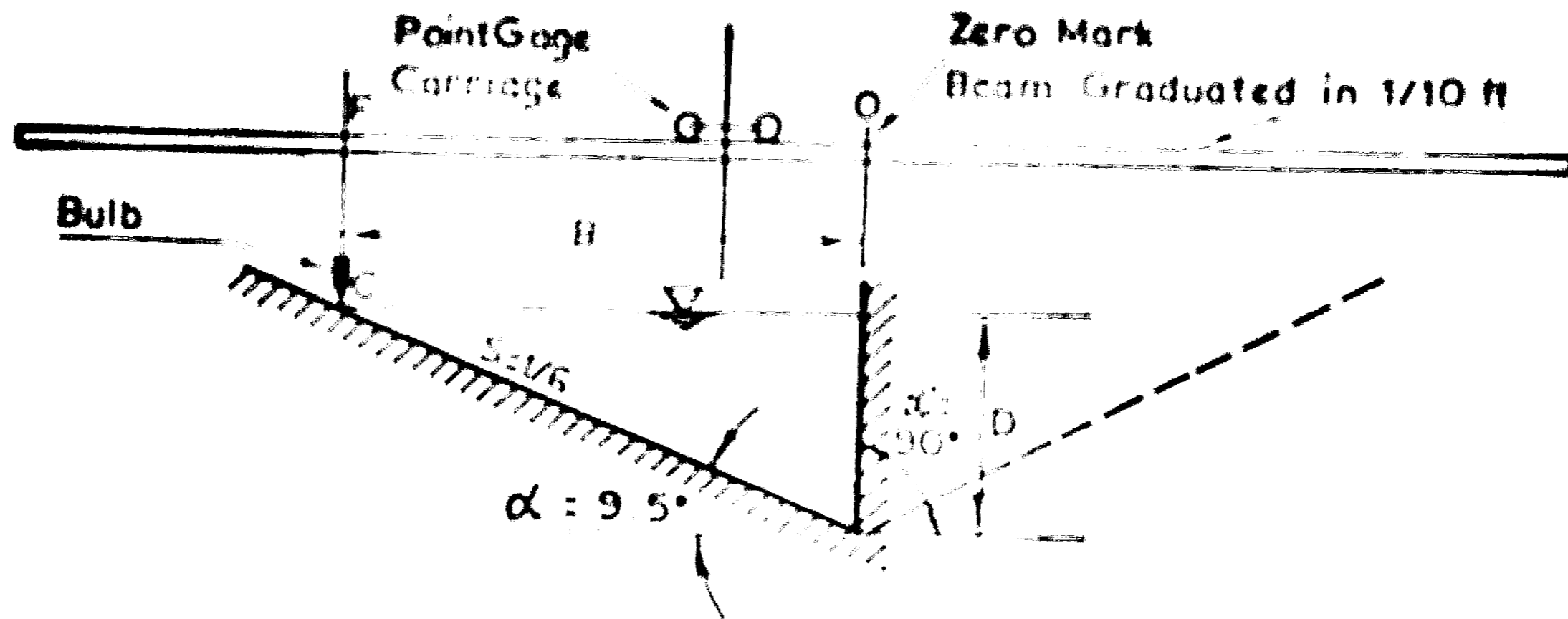
Fig. 3.3: Depth and Width Measurements for Triangular Flume With Longitudinal Wall
(Not to Scale)
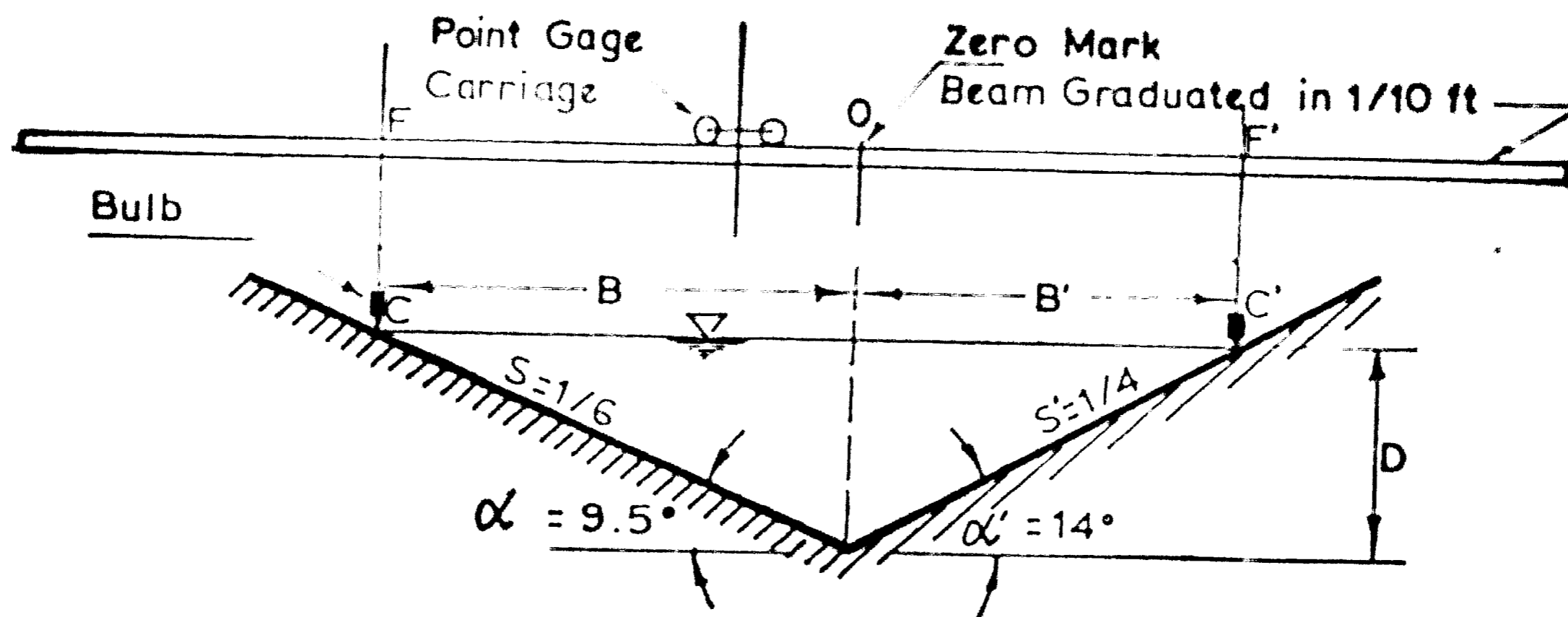
Fig. 3.4: Depth and Width Measurements for Triangular Flume Without Longitudinal Wall
(Not to Scale)

α or α', and the widths, B or B'. The angles, α and α', the widths, B and B', and the slope, S_o, were measured at every foot within the chosen reach.

To utilize both, namely, the direct depth measurements and the (indirect) depth calculations, the following procedure for the computation of the average depths was adopted:

-26-

$$\overline{D} = \frac{D + B \tan \alpha + B' \tan \alpha'}{3} \qquad (3.2)$$

where D is the measured depth and B and B' are the measured widths.

Width Measurements: The widths, B or B', varying with discharge, were measured directly by using the plumb bob. The plumb bob was lowered from the transversal beam graduated in tenths of a foot, shown in Figs. 3.3 and 3.4, down to the points, E or E', where the free water surface and the side slopes met. The marks at F or at F' were read off and the distances, $\overline{Fo}$ or $\overline{F'o}$, were known at once. This method was repeated for all cross sections.

Tables A-4 and A-5 in Appendix A summarize the data and computation for the triangular flume without and with the longitudinal wall, respectively.

4. EVALUATION OF THE EXPERIMENTAL DATA

4.1 Computation of Uniform Depth for Both Rectangular and Triangular Channels

The uniform depth for a given discharge was computed as follows:

(1) The average depth of each cross section, D_i, was computed for a rectangular flume as (see Eq. (3.1))

$$\bar{D}_i = \frac{D_1 + D_2 + D_3}{3} \qquad (4.1)$$

for a rectangular flume as (see Eq. (3.2))

$$D_i = \frac{D + B \tan \alpha + B' \tan \alpha'}{3} \qquad (4.2)$$

(2) Once the cross-sectional depths, $\bar{D}_i$, given by Eq. (4.1) or Eq. (4.2), were available, the channel's mean uniform depth, D_u, for a carefully chosen uniform reach (see Fig. 4.1) - this one was as far as possible removed from the entrance and exit zones - was calculated as

$$D_u = \frac{\sum_1^N D_i}{N} \qquad (4.3)$$

4.2 Computation of Various Hydraulic Parameters

4.2.1 Rectangular Channel

<u>Cross Section Area, A</u>: The cross section area was computed accordingly:

-28-
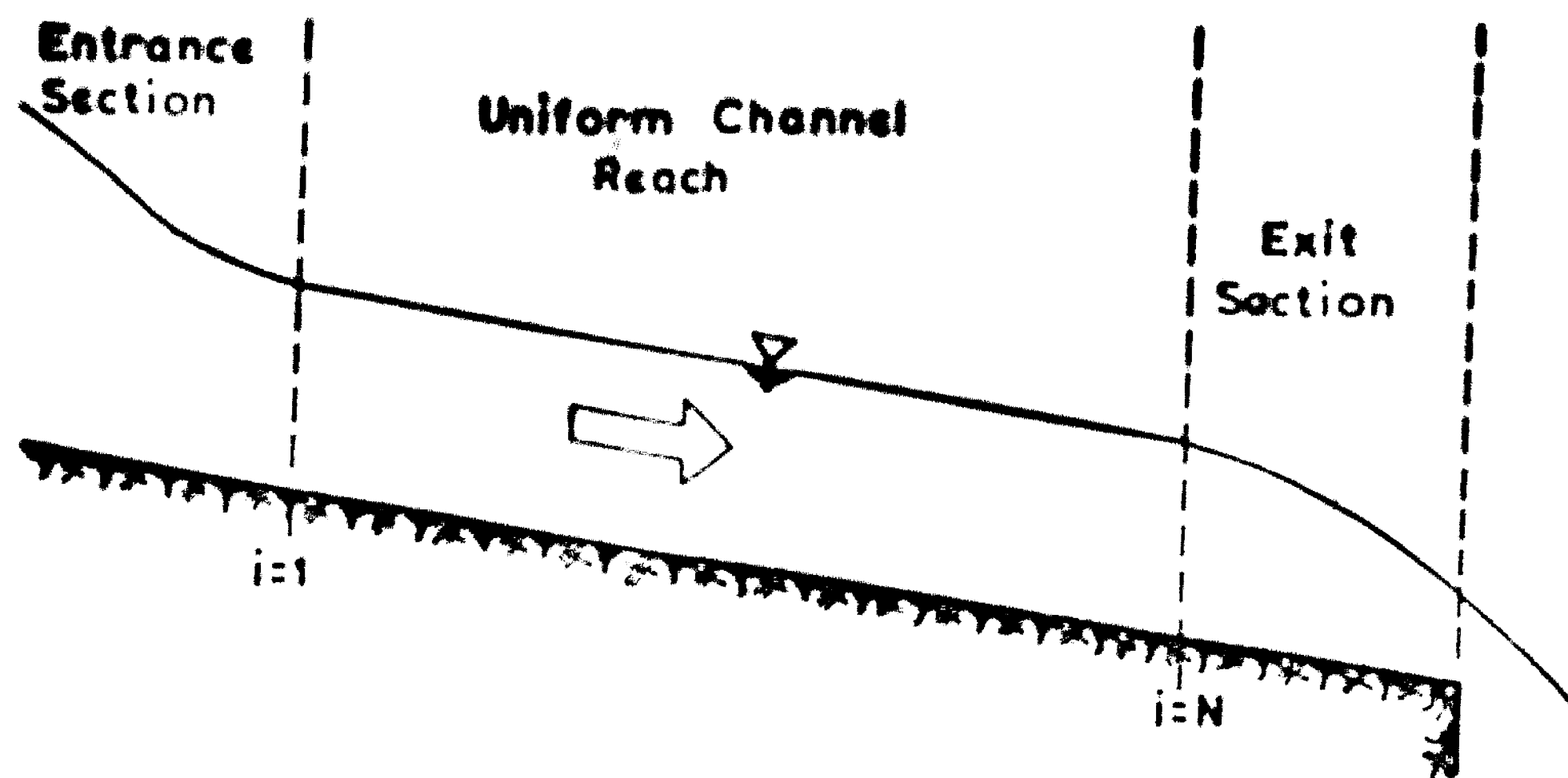
Fig. 4.1: Sketch of the Uniform Flow Definition

$$A = D_u \cdot B \qquad (4.4)$$

where D_u is the uniform depth and B is the constant width of the glass-walled flume.

Average Velocity of the Flow, $\bar{u}$: The expression of the velocity of the flow reads

$$\bar{u} = \frac{Q}{A} \qquad (4.5)$$

where Q is the flow rate computed according to Eq. (2.1) and A is the cross section area given by Eq. (4.4).

Hydraulic Radius with Respect to the Entire Cross Section, R_h: The hydraulic radius was computed by

$$R_h = \frac{A}{B + 2D_u} \qquad (4.6)$$

where A is the area given by Eq. (4.4) and B and D_u are the width of the channel and the uniform depth.

Reynolds Number, N_R: The Reynolds number of the flow was calculated according to the general formula which reads

$$N_R = \frac{4 R_h \bar{u}}{\nu} \qquad (4.7)$$

in which ν is the kinematic viscosity of the flowing water.

Hydraulic Radius Pertaining to the Wall, R_w: Figure 4.2 shows the cross section with different roughnesses; the roughness of the two sides is different from the roughness of the bed of the flume. In the case of a cross section with different roughnesses, the individual roughnesses are added to form the equivalent roughness of the entire cross section.

The computation of the composite roughness is reviewed by CHOW (1959, p. 136). It is assumed that the entire cross section is divided into units; that is, into a finite number of the cross sections corresponding to the materials which form the wetted perimeter, as can be seen in Fig. 4.2. An additional assumption is that the average velocity given by Eq. (4.5) is the same at every unit of the cross section. Based on the above assumptions, the flow computation for each unit can be made. Furthermore, the hydraulic radius of each unit can

-30-
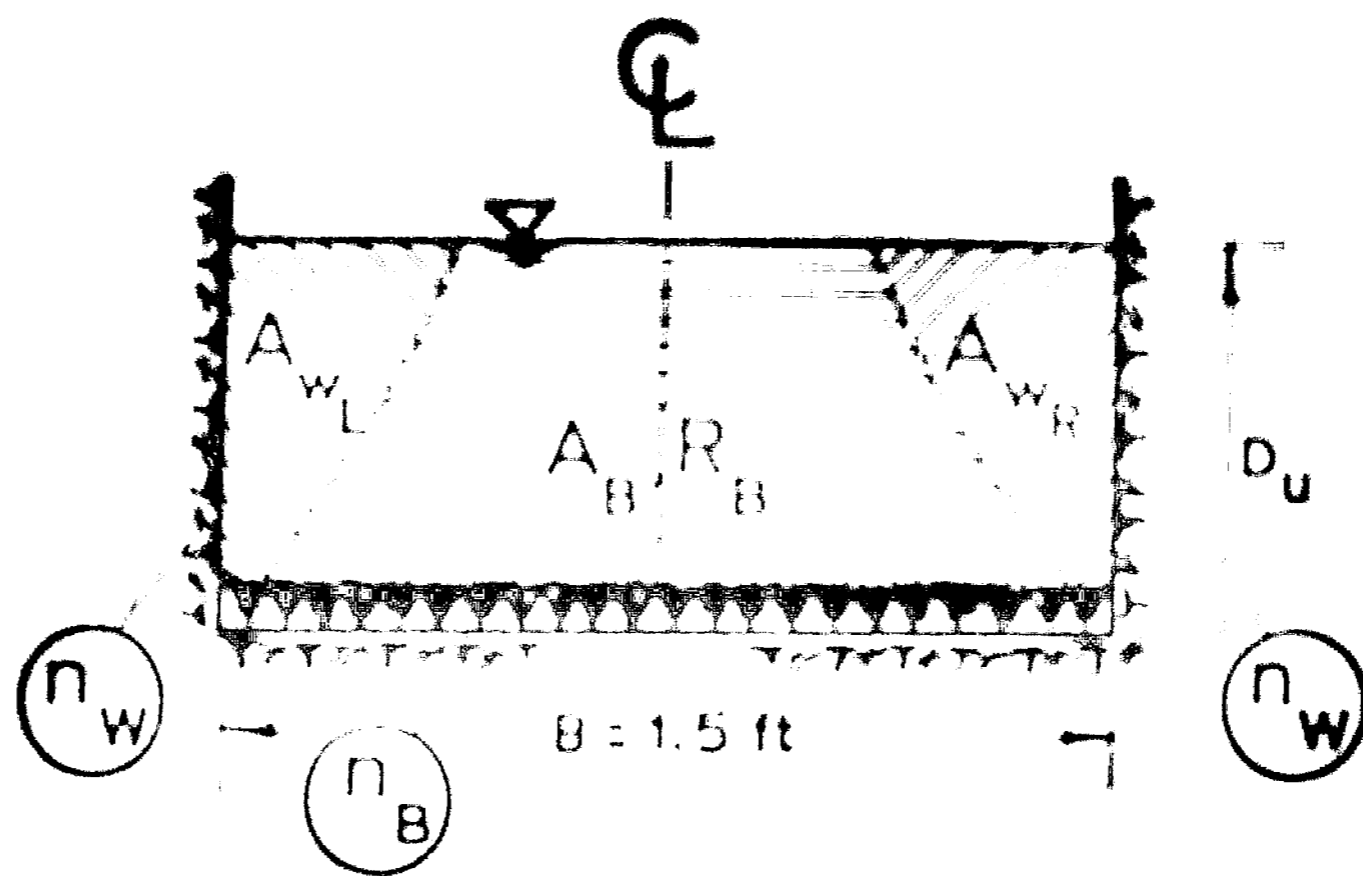
Fig. 4.2: Elements of the Cross Section

be expressed in terms of the roughness coefficient, n, the average velocity, $\bar{u}$, and the slope of the uniform flow, S_o, as shown by the Manning formula. If n_w^* is the known value of the roughness coefficient of the wall unit, the hydraulic radius, R_w, pertaining to the wall is

$$R_w = \frac{n_w}{1.486} \cdot \frac{\bar{u}}{S_o^{0.5}} \qquad (4.8)$$

<u>Area Pertaining to the Wall, A_w</u>: As can be seen in Fig. 4.2, the areas, A_{w_L} and A_{w_R}, are added together provided that the side walls are made of the same materials; that is,

$$A_w = A_{w_L} + A_{w_R} \qquad (4.9)$$

---

[*] For the glass-wall an n-value of $n_w = 0.01$ was taken from CHOW (1959, p. 110).

Since Fig. 4.2 is symmetrical about its center line, the areas, A_{w_L} and A_{w_R}, are equal. With this information, the following equation reads

$$A_w = 2 (P_w R_w) \qquad (4.10)$$

It can be seen in Fig. 4.2 that the wetted perimeter, P_w, with respect to each wall is the flow depth, D_u. So Eq. (4.10) becomes

$$A_w = 2 (D_u R_w) \qquad (4.11)$$

Area Pertaining to the Bottom, A_B: With reference to Fig. 4.2, the area, A_B, with respect to the channel bottom is the difference between the whole area, A, given by Eq. (4.4), and the area given by Eq. (4.11). The expression of the bottom area is then written as

$$A_B = D_u B - 2 (D_u R_w) \qquad (4.12)$$

Hydraulic Radius Pertaining to the Bottom, R_B: With the knowledge of Eq. (4.12), the following expression is obtained, provided that the wetted perimeter pertaining to the bottom is $P_w = B$.

$$R_B = \frac{A_B}{B} = D_u \cdot \left[1 - 2 \frac{R_w}{B} \right] \qquad (4.13)$$

4.2.2 Triangular Channels

Widths of the Channels, B and B': The uniform widths, B and B', (see Tables A-4 and A-5, Appendix A) were computed as follows for the known uniform depth, D_u:

-32-

$$B + B' = \left[\frac{1}{\tan \alpha} + \frac{1}{\tan \alpha'} \right] D_u \qquad (4.14)$$

Cross-Sectional Area, A: The cross-sectional area was calculated according to

$$A = \left[\frac{1}{\tan \alpha} + \frac{1}{\tan \alpha'} \right] \frac{D_u^2}{2} \qquad (4.15)$$

Average Velocity, $\bar{u}$: With the knowledge of Eq. (4.15) the average velocity, $\bar{u}$, was computed according to Eq. (4.5).

Wetted Perimeter, P: The following equation was used to compute the wetted perimeter:

$$P = \left[\frac{1}{\sin \alpha} + \frac{1}{\sin \alpha'} \right] D_u \qquad (4.16)$$

Hydraulic Radius, R: With the results of Eqs. (4.15) and (4.16) the hydraulic radius, R, was computed as

$$R_h = \frac{A}{P} \qquad (4.17)$$

Reynolds Number, N_R: The same formula given by Eq. (4.7) was used to compute the Reynolds number, N_R.

4.3 Computation of the Bottom Roughness Coefficient

4.3.1 Rectangular Channel

Both the roughness coefficients, $n_{A.1}$ and $n_{A.2}$, of Astroturf No. 1 and Astroturf No. 2, respectively, and of wood, n_{wood}, were obtained by a modified Manning relation:

$$n_B = \frac{1.468}{\bar{u}} \cdot R_B^{0.67} \cdot S_o^{0.5} \tag{4.18}$$

where $\bar{u}$ and R_B are computed according to Eqs. (4.5) and (4.13), respectively. Equation (4.18) is based on the same assumption as Eq. (4.8).

4.3.2 Triangular Channels

Since the wetted perimeter of the triangular channels is composed of one single roughness (Astroturf No. 1), the roughness coefficient, $n_{A \cdot 1}$, was calculated according to

$$n_{A \cdot 1} = \frac{1.486}{\bar{u}} \cdot R_h^{0.67} \cdot S_o^{0.5} \tag{4.19}$$

where $\bar{u}$ and R_h are computed by Eqs. (4.5) and (4.17), respectively.

4.4 Sample Calculation

An example best illustrates the foregoing steps.

4.4.1 Rectangular Channel

For the following sample calculations, the reader is referred to the first line of Table A-1, Appendix A, column by column.

(1) The kind of roughness was specified as "Astroturf No. 1". The summary of sizes of Astroturf No. 1 is given in Table 2.1.

(2) The longitudinal slope, S_o, was set according to the procedure given in Section 3.1. It was $S_o = 0.0176$.

-34-

(3) The air-water manometer deflection, ΔH, was read off as $\Delta H = 3.470$ ft.

(4) Equation (2.1) was used and

$$Q = 1.05 \cdot (3.47)^{0.522} = 1.98 \text{ ft}^3/\text{sec}$$

(5) The depth, D_u, for the uniform channel reach (see Fig. 4.1) was calculated by using the accuracy calculation. The error of the difference in n-roughness values computed from two mean cross-sectional depths given by Eq. (4.1) must be within the adopted range[*]. If the accuracy of the difference computed from two different depths, $\overline{D}_i$, is within the allowable error, the uniform depth, D_u, is the average of all cross-sectional depths bounded by these two depths, $\overline{D}_i$. According to the above procedure, the resulting uniform depth was found to be 0.416 ft.

(6) The area, A, of the cross section was calculated according to Eq. (4.4):

$$A = 0.416 \cdot 1.5 = 0.624 \text{ ft}^2$$

(7) Equation (4.5) was used to compute the mean velocity, $\overline{u}$, of the flow; that is,

---

[*]If a is called the accuracy of the difference in n values, the following inequalities were adopted for different ranges of discharges:

High discharges: $10\% < a \leq 15\%$
Medium discharges: $5\% < a \leq 10\%$
Lower discharges: $0\% \leq a \leq 5\%$

$$\bar{u} = \frac{1.98}{0.624} = 3.173 \text{ ft/sec}$$

(8) The hydraulic radius, R_h, of the cross section was obtained by Eq. (4.6):

$$R_h = \frac{0.624}{1.5 + 2 \cdot (0.416)} = 0.268 \text{ ft}$$

(9) The Reynolds number, N_R, of the flow was calculated according to Eq. (4.7), provided that the kinematic viscosity of the flow at $70°F$ is equal to $1.059 \times 10^{-5} \text{ ft}^2/\text{sec}$[*]; that is,

$$N_R = \frac{4 \cdot (0.268) \cdot (3.173)}{1.059 \cdot (10^{-5})} = 320,700 = 3.2 \times 10^5$$

(10) With the roughness coefficient of the walls ($n_w = 0.01$), the hydraulic radius pertaining to the walls, R_w, was according to Eq. (4.8)

$$R_w = \left[\frac{0.01}{1.486} \cdot \frac{3.173}{(0.0176)^{0.5}} \right]^{1.5} = 0.064 \text{ ft}$$

(11) By using Eq. (4.11) the area pertaining to the walls, A_w, was obtained

$$A_w = 2 \cdot (0.416 \cdot 0.064) = 0.054 \text{ ft}^2$$

(12) The area of the cross section, A_B, pertaining to the bottom of the flume was computed according to Eq. (4.12); that is,

---

[*]The kinematic viscosity of water, ν, depending on the temperature, is given by OLSON (1970, p.21)

$$A_B = 0.416 \cdot 1.5 - 2 \,(0.416 \cdot 0.064) = 0.570 \text{ ft}^2$$

(13) The hydraulic radius pertaining to the bottom of the flume, R_B, was calculated according to Eq. (4.13):

$$R_B = 0.416 \cdot \left[1 - 2 \cdot \frac{0.064}{1.5}\right] = 0.380 \text{ ft}$$

(14) Finally, the value of the roughness coefficient, $n_{A \cdot 1}$, of Astroturf No. 1 was, according to Eq. (4.18), for $N_B = n_{A \cdot 1}$

$$n_{A \cdot 1} = \frac{1.486}{3.173} \cdot (0.38)^{0.67} \cdot (0.0176)^{0.5} = 0.033$$

4.4.2 Triangular Channel

For the following sample calculations, the reader is referred to the first line of Table A-5 in Appendix A column by column.

(1) Astroturf No. 1 was investigated.

(2) The longitudinal slope, S_o, of the triangular channel was set according to the procedure described in Section 3.2. It was 0.027.

(3) The liquid-water manometer deflection, ΔH, was read off as $\Delta H = 4.760$ ft.

(4) The discharge, Q, was computed according to Eq. (2.2); that is,

$$Q = 0.42 \cdot (4.76)^{0.5} = 2.95 \text{ ft}^3/\text{sec}$$

(5) The computation of the uniform depth, D_u, for the triangular channel was the same as that of the rectangular channel. Based on that procedure, the resulting uniform depth was

$$D_u = 0.583 \text{ ft}$$

(6) The width of the uniform flow, B, was computed according to Eq. (4.14). For the cross section with longitudinal wall, i.e., $\alpha' = 90^O$ and $\tan \alpha' = \infty$, Eq. (4.14) reduces to

$$B = \frac{1}{\tan \alpha} \cdot D_u; \quad \alpha = 9.5^O$$

or

$$B = \frac{1}{0.1673} \cdot 0.583 = 3.370$$

(7) The cross-sectional area, A, was calculated by means of Eq. (4.15) which can be reduced to

$$A = \frac{1}{\tan \alpha} \cdot \frac{D_u^2}{2}$$

for the case of a triangular flume with longitudinal wall; i.e., $\alpha' = 90^O$ and $\tan \alpha' = \infty$. So the value of A was

$$A = \frac{1}{0.1673} \cdot \frac{(0.583)^2}{2} = 0.982 \text{ ft}^2$$

(8) Equation (4.5) was used to compute the average velocity, $\bar{u}$, of the flow; that is,

$$\bar{u} = \frac{2.95}{0.982} = 3.003 \text{ ft/sec}$$

-38-

(9) Equation (4.16) reduces in the present case to:

$$P = \left[\frac{1}{\sin \gamma} + 1 \right] D_u$$

since $\alpha' = 90^\circ$ and $\sin \alpha' = 1$. This simplified formula was used to compute the wetted perimeter, P; that is,

$$P = \left[\frac{1}{0.165} + 1 \right] 0.583 = 4.116 \text{ ft}$$

(10) To compute the hydraulic radius, R_h, Eq. (4.17) was used:

$$R_h = \frac{0.982}{4.116} = 0.239 \text{ ft}$$

(11) The Reynolds number, N_R, according to Eq. (4.7), was

$$N_R = \frac{4 \cdot 0.239 \cdot 3.003}{1.059 \cdot 10^{-5}} = 2.707 \cdot 10^5$$

(12) Finally, the roughness coefficient, $n_{A \cdot 1}$, of Astroturf No. 1 was, according to Eq. (4.19),

$$n_{A \cdot 1} = \frac{1.486}{3.003} \cdot (0.239)^{0.67} \cdot (0.027)^{0.5} = 0.031$$

5. REPRESENTATION OF DATA

The computed roughness coefficients, n, were plotted against
the respective uniform flow depths, D_u, and the Reynolds numbers, N_R,
in Figs. 5.1 and 5.2, respectively. Both plots show the same general
trend of the three curves, which is found in overall agreement with
Lane's results (1951) reported by CHOW (1959) and given in Fig. 1.2.

The curves for the wooden surface are reasonably vertical.
Figures 5.1 and 5.2 show that the n-value for both Astroturfs increases
as the flow depth and/or the Reynolds number decreases. This can be ex-
plained by the fact that the exposure of Astroturf is more and more pro-
nounced as the depth and/or Reynolds number decreases. This can also
be seen in Fig. 5.3, where the depth to Astroturf's height ratio is
plotted against the n-value. However, the curves of Figs. 5.1 and 5.2
show a reasonable independency of the n-value at the high range of
depths and Reynolds numbers. In other words, the n-value no longer
depends upon the depth of the flow and the Reynolds number, but becomes
a constant value.
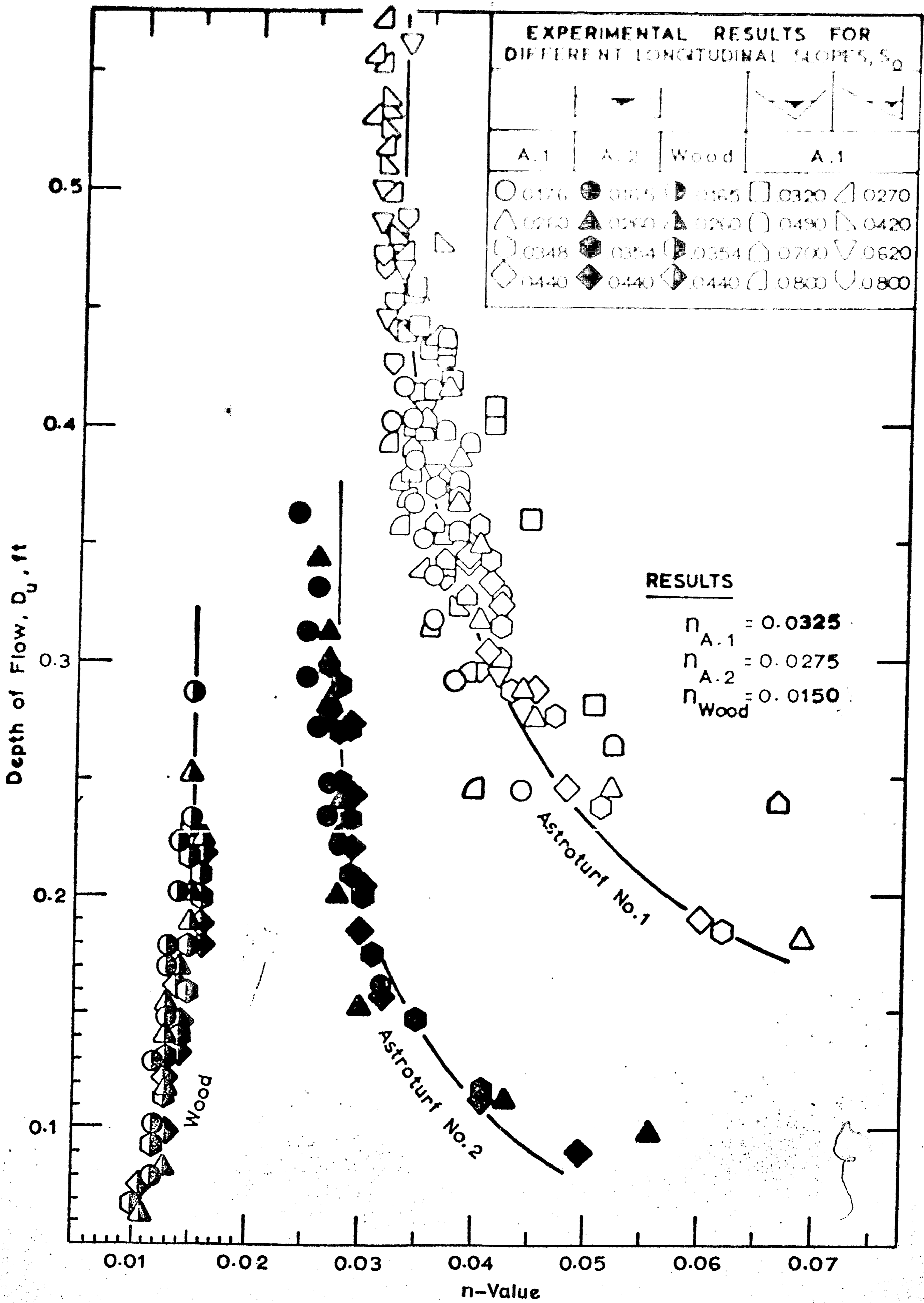
Fig. 5.1   Variation of n–Value With Depth, D_u

-41-
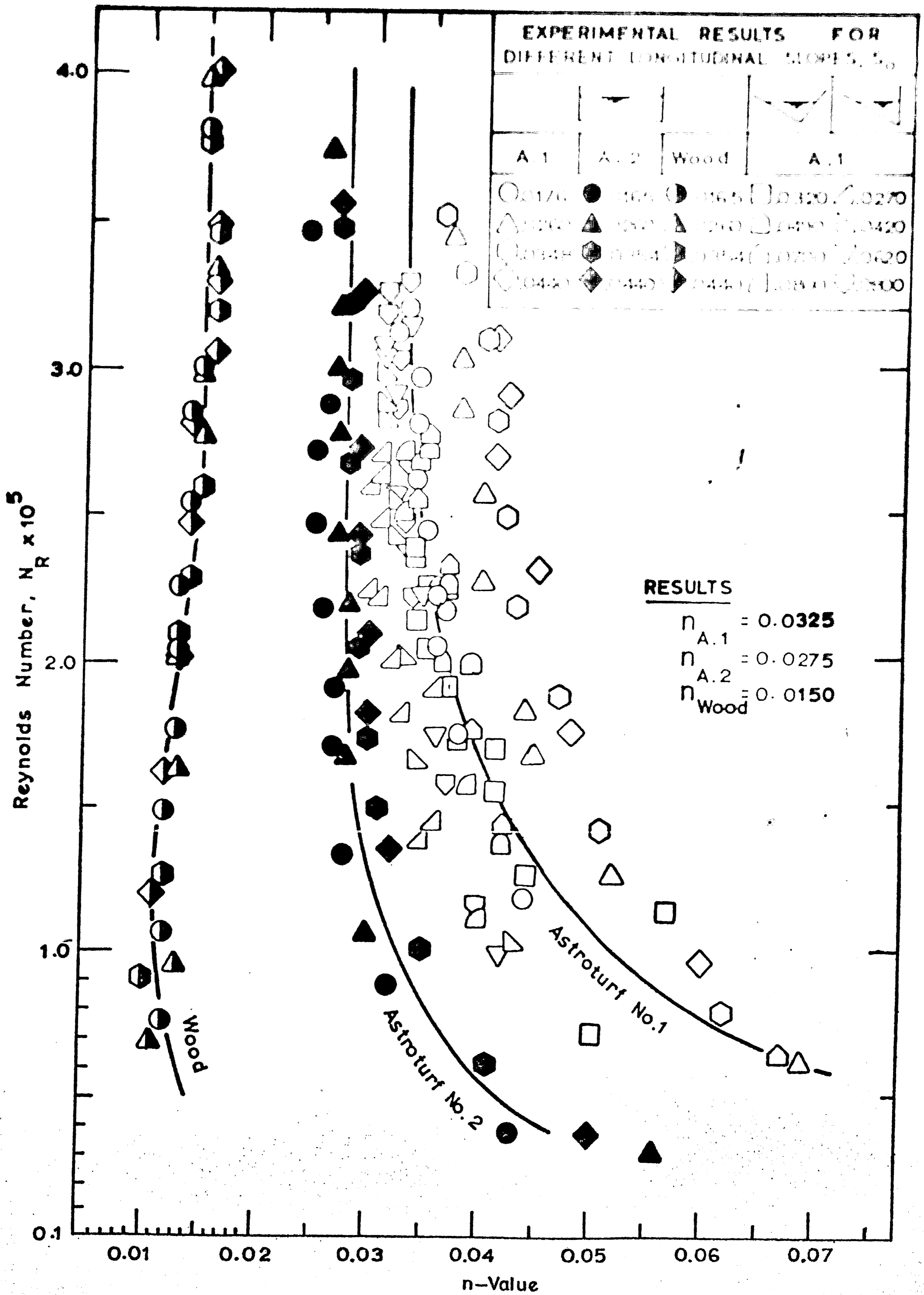
Fig. 5.2 Reynolds Number Versus Roughness Coefficient

-42-
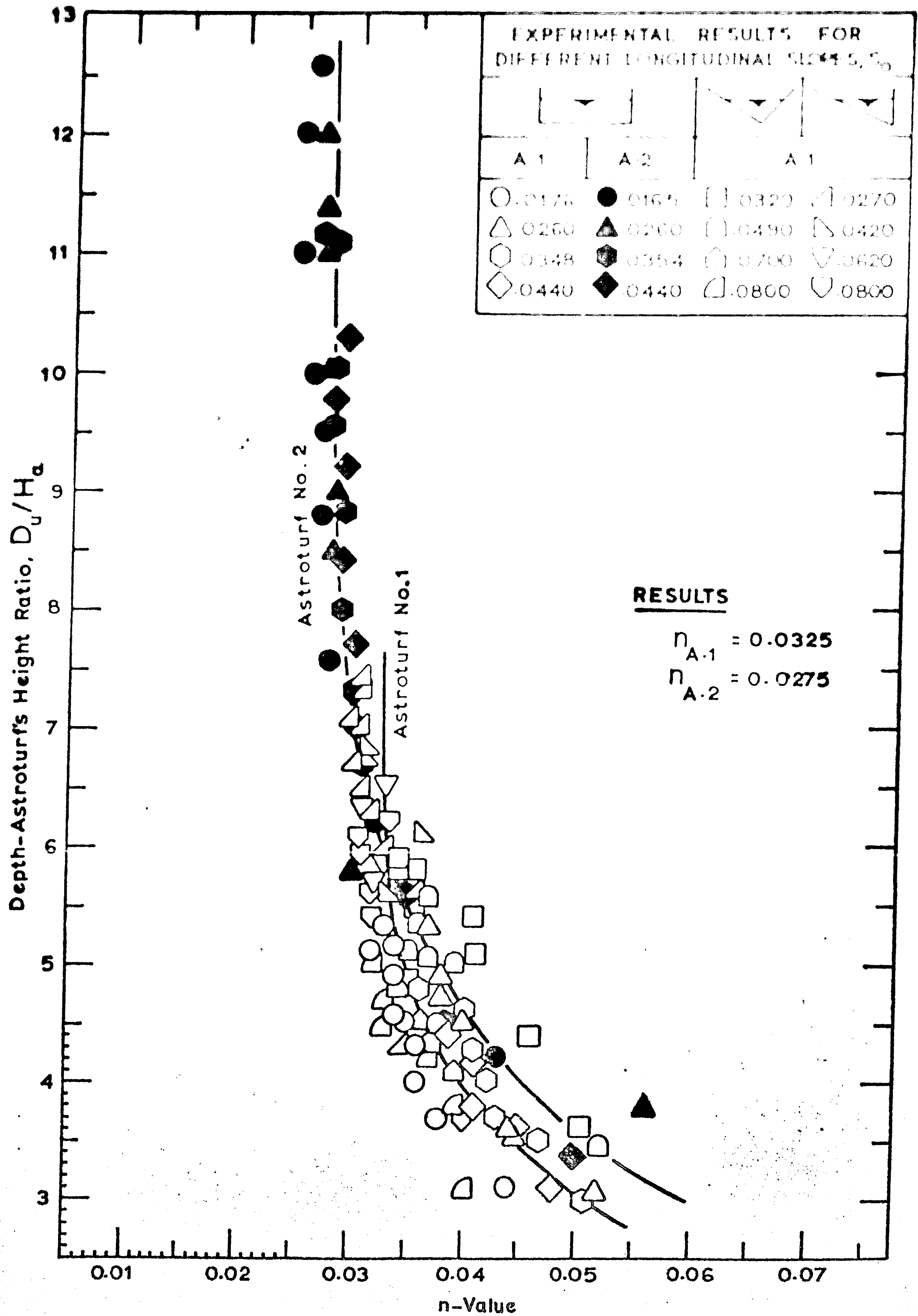
Fig. 5.3 Variation of n-Value With Depth-Astroturf's Height Ratio, D_u/H_a

6. CONCLUDING REMARKS

The roughness of two types of artificial grass, Astroturf No. 1 and Astroturf No. 2, have been investigated in three different hydraulic flumes. The following conclusions can be drawn from the present study.

The n-value was found to be dependent on the flow depth and on the Reynolds number at low range of depths. It was shown to be independent of the flow parameters at high range of depths.

It seems reasonable to select the roughness coefficient for the range of the higher discharges as constant, being

$$n_{A \cdot 1} = 0.0326 \quad \text{for Astroturf No. 1,}$$

$$n_{A \cdot 2} = 0.0275 \quad \text{for Astroturf No. 2, and}$$

$$n_{wood} = 0.0150 \quad \text{for the wooden surface.}$$

Table 6.1 shows a comparison of Manning's roughness coefficients for "real" grass and for "model" grass, i.e., for Astroturf. In this table the ranges of n-values for high and short "real" grass were taken from Table 1.1; while for "model" grass, the results of the present experiment are used.

Manning's Roughness Coefficient, n	
"Real" Grass	"Model" Grass [Astroturf]
High Grass 0.030 — 0.050	Astroturf No. 1 $n_{A \cdot 1} = 0.0325$
Short Grass 0.025 — 0.035	Astroturf No. 2 $n_{A \cdot 2} = 0.0275$

Table 6.1: Comparative n-values

-44-

From the above table we may conclude that Astroturf, being a "model" grass, simulates reasonably well the "real" grass.

We recommend the use of Astroturf in the simulation of grass in hydraulic modeling.

7. IMPORTANCE OF STUDY TO HYDRAULIC MODELING

To illustrate the usefulness of having a "model" grass available, we shall perform a numerical example.

Simulating a grassed watercourse, it becomes necessary to consult a frictional criterion, as discussed by GRAF (1971, p. 389) and YEE (1972, pp. 13-14).

Equation (1.1), which is the Manning empirical relationship, may be used as a frictional criterion. This frictional criterion requires a relationship between prototype and model[*] such as

$$\left[\frac{R_h^{2/3} S_o^{1/2}}{\bar{u} \cdot n} \right]_p = \left[\frac{R_h^{2/3} S_o^{1/2}}{\bar{u} \cdot n} \right]_m \tag{7.1}$$

for an undistorted model, $(S_o)_p = (S_o)_m$. If the hydraulic radius is replaced by a suitable dimension, L, Eq. (7.1) reduces to

$$\left[\frac{L^{2/3}}{\bar{u} \cdot n} \right]_p = \left[\frac{L^{2/3}}{\bar{u} \cdot n} \right]_m \tag{7.2}$$

Equation (7.2) can be rearranged for the discharge relationship; that is,

$$\frac{Q_p}{Q_m} = \left[\frac{L_p}{L_m} \right]^{2.67} \cdot \frac{n_m}{n_p} \tag{7.3}$$

---

[*]The letters p and m will stand for prototype and model, respectively.

EXAMPLE

A grass-lined irrigation canal is to be investigated in the hydraulic laboratory. An undistorted model with a scale ratio of $\frac{L_p}{L_m} = \frac{10}{1}$ is to be built. The laboratory pump system provides a maximum discharge (i.e., model discharge) of $Q_m^{max} = 3$ cfs. For what maximum discharge, Q_p^{max}, of the irrigation canal, having $n_p = 0.030$, is this laboratory investigation applicable?

ANSWER

Use of Eq. (7.3):

(α) Laboratory Investigation with Wood

$$n_{wood} = 0.0150$$

$$Q_p = \left[\frac{10}{1}\right]^{2.67} \cdot \frac{0.0150}{0.030} \cdot Q_m = 165\ Q_m \qquad (7.3)$$

$$Q_p^{max} = 165.3 = \underline{495\ cfs}$$

(β) Laboratory Investigation with Astorturf No. 1

$$n_{A\cdot 1} = 0.0325$$

$$Q_p = \left[\frac{10}{1}\right]^{2.67} \cdot \frac{0.0325}{0.030} \cdot Q_m = 510\ Q_m \qquad (7.3)$$

$$Q_p^{max} = 510.3 = \underline{1530\ cfs}$$

(γ) Laboratory Investigation with Astroturf No. 2

$$n_{A\cdot 2} = 0.0275$$

$$Q_p = \left[\frac{10}{1}\right]^{2.67} \cdot \frac{0.0275}{0.030} \cdot Q_m = 430\ Q_m \qquad (7.3)$$

$$Q_p^{max} = 430.3 = \underline{1290\ cfs}$$

-47-

Length Scale $L_p/L_m = 10/1$			
Model		Prototype	
Q_m^{max}, ft^3/sec	n_m	Q_p^{max}, ft^3/sec	n_p
	$n_{A\cdot 1} = 0.032?$	1530	
3	$n_{A\cdot 2} = 0.027?$	1290	0.030
	$n_{wood} = 0.0150$	495	

Table 7.1: Summary of Example Results

From the above example, we shall conclude that:

(a) Our hydraulic laboratory cannot model any prototype canal which carries a maximum discharge greater than 1530 cfs, 1290 cfs, and 495 cfs for laboratory investigation with Astroturf No. 1, with Astroturf No. 2, and with the wooden surface, respectively.

(b) In order to model any prototype canal carrying very high discharge, a material of high roughness coefficient, such as Astroturf, is recommended to be used in modeling.

APPENDIX A
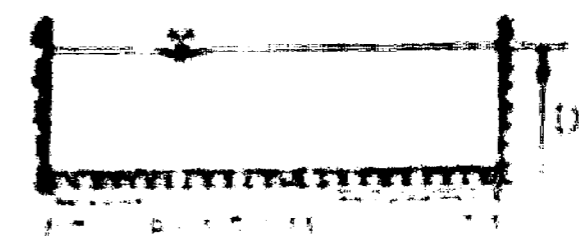## SUMMARY OF DATA AND COMPUTATION

TABLE A·1   SUMMARY OF DATA AND COMPUTATION

KIND OF BEDLINING	DATA		COMPUTATION										
	S_o	ΔH (ft)	Q (ft³/sec)	D_u (ft)	A (ft²)	(ft/sec)	R_x (ft)	N_e	D_w (ft)	A_w (ft²)	A_B (ft²)	R_B (ft)	$n_{A?}$
1	2	3	4	5	6	7	8	9	10	11	12	13	14
No.1	.0170	3.470	1.982	.416	.625	3.877	.248	3.237E+05	.055	.045	.573	.383	.033
	.0170	3.110	1.805	.423	.633	3.858	.241	3.100E+05	.056	.042	.552	.367	.032
	.0170	2.870	1.837	.423	.636	3.743	.242	2.905E+05	.053	.040	.557	.372	.034
	.0170	2.360	1.683	.385	.577	3.515	.236	2.653E+05	.057	.039	.515	.346	.034
	.0170	2.300	1.543	.364	.543	3.033	.240	2.443E+05	.055	.034	.512	.342	.035
	.0170	1.770	1.413	.352	.527	3.043	.242	2.562E+05	.052	.035	.508	.323	.035
	.0170	1.474	1.270	.339	.505	3.534	.232	2.205E+05	.054	.031	.473	.315	.036
	.0170	1.200	1.155	.317	.476	2.623	.227	2.058E+05	.043	.027	.443	.299	.036
	.0170	.847	.955	.291	.437	2.196	.210	1.757E+05	.037	.022	.415	.277	.039
	.0170	.504	.726	.265	.367	1.703	.185	1.138E+05	.025	.012	.355	.237	.044
ASTROTURF	.0260	3.850	2.127	.415	.622	3.859	.247	3.443E+05	.254	.045	.572	.385	.037
	.0260	2.970	1.871	.385	.577	3.353	.256	3.009E+05	.049	.037	.542	.361	.033
	.0260	2.570	1.757	.366	.549	3.306	.256	2.590E+05	.044	.034	.515	.344	.038
	.0260	1.960	1.591	.350	.525	2.941	.233	2.421E+05	.041	.029	.495	.331	.040
	.0260	1.440	1.279	.316	.474	2.693	.222	2.126E+05	.035	.024	.450	.306	.043
	.0260	.915	1.000	.288	.432	2.314	.205	1.553E+05	.033	.017	.415	.276	.044
	.0260	.765	.910	.275	.412	2.206	.201	1.677E+05	.024	.015	.397	.266	.045
	.0260	.415	.659	.246	.369	1.787	.185	1.250E+05	.020	.010	.357	.239	.052
	.0260	.090	.299	.191	.271	1.120	.146	6.359E+04	.010	.004	.265	.179	.069
	.0260	.030	.168	.147	.271	.764	.123	3.546E+04	.006	.002	.219	.146	.087
	.0348	3.740	2.090	.371	.555	3.756	.248	3.522E+05	.050	.037	.519	.346	.036
	.0348	3.340	1.971	.369	.553	3.560	.247	3.326E+05	.046	.034	.520	.346	.038
	.0348	2.860	1.817	.358	.537	3.384	.242	3.097E+05	.043	.031	.506	.338	.040
	.0348	2.320	1.629	.341	.512	3.181	.235	2.419E+05	.039	.027	.486	.324	.041
	.0348	1.735	1.398	.314	.471	2.968	.221	2.441E+05	.035	.022	.449	.299	.042
	.0348	1.265	1.195	.289	.433	2.756	.209	2.171E+05	.031	.018	.415	.277	.043
	.0348	.940	1.017	.277	.415	2.447	.202	1.800E+05	.026	.015	.401	.267	.047
	.0348	.510	.739	.238	.357	2.069	.181	1.412E+05	.020	.010	.347	.232	.051
	.0348	.150	.390	.193	.274	1.421	.147	7.894E+04	.012	.004	.273	.180	.052
	.0348	.010	.136	.113	.169	.504	.098	2.951E+04	.005	.001	.168	.112	.060
	.0440	3.300	1.958	.346	.519	3.773	.237	3.374E+05	.042	.029	.490	.327	.039
	.0440	3.250	1.943	.343	.514	3.776	.235	3.357E+05	.042	.029	.486	.324	.039
	.0440	3.270	1.549	.344	.516	3.777	.236	2.366E+05	.042	.029	.487	.325	.039
	.0440	2.740	1.777	.333	.499	3.558	.231	3.099E+05	.039	.026	.474	.316	.041
	.0440	2.380	1.651	.324	.486	3.397	.226	2.903E+05	.036	.023	.463	.309	.042
	.0440	1.980	1.500	.302	.453	3.311	.215	2.693E+05	.035	.021	.432	.288	.041
	.0440	1.430	1.266	.286	.429	2.956	.207	2.307E+05	.029	.017	.412	.275	.045
	.0440	.760	.922	.245	.367	2.510	.185	1.751E+05	.023	.011	.356	.238	.048
	.0440	.225	.476	.189	.284	1.680	.151	9.582E+04	.013	.005	.279	.186	.060
	.0440	.350	.220	.142	.213	1.032	.119	4.654E+04	.006	.002	.211	.141	.082
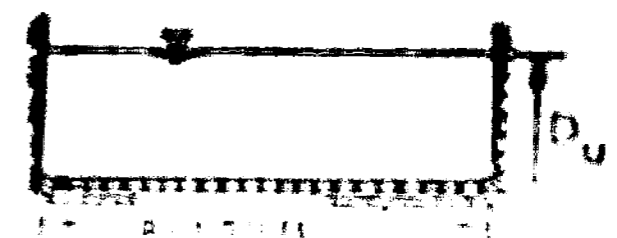
TABLE A·2 SUMMARY OF DATA AND COMPUTATION

KIND OF ...	DATA		COMPUTATION										
	S_0	ΔH (ft)	Q (ft³/sec)	D_2 (ft)	A (ft²)	V (ft/sec)	R	N_R	H (ft)	A_m (ft²)	A_B (ft²)	R_B (ft)	n A.2
1	2	3	4	5	6	7	8	9	10	11	12	13	14
ASTROTURF No. 2	.0160	3.200	2.346	.363	.544	3.758	.245	3.473E+05	.087	.053	.485	.323	.024
	.0160	2.743	1.943	.332	.495	3.518	.229	2.958E+05	.072	.048	.447	.298	.024
	.0160	2.213	1.722	.301	.455	3.567	.223	2.725E+05	.072	.044	.423	.282	.025
	.0160	1.643	1.500	.269	.429	3.225	.213	2.395E+05	.066	.038	.402	.271	.025
	.0160	1.243	1.273	.244	.372	2.983	.192	2.135E+05	.059	.032	.355	.254	.026
	.0160	.925	1.205	.244	.372	2.733	.186	1.827E+05	.053	.026	.345	.232	.027
	.0160	.620	.885	.232	.345	2.542	.170	1.557E+05	.044	.023	.323	.211	.027
	.0160	.415	.663	.200	.300	2.223	.165	1.027E+05	.042	.023	.307	.197	.027
	.0160	.192	.429	.163	.245	1.755	.135	1.057E+05	.032	.023	.254	.167	.032
	.0160	.033	.168	.111	.167	1.011	.057	7.048E+04	.017	.021	.155	.107	.043
ASTROTURF	.0260	4.700	2.171	.347	.519	4.713	.235	3.751E+05	.074	.045	.464	.309	.026
	.0260	2.930	1.827	.313	.472	3.969	.221	3.211E+05	.065	.040	.424	.290	.027
	.0260	2.430	1.649	.300	.450	3.709	.214	3.002E+05	.061	.037	.419	.278	.027
	.0260	2.060	1.527	.284	.426	3.576	.205	2.742E+05	.058	.037	.393	.262	.027
	.0260	1.625	1.297	.257	.385	3.366	.191	2.435E+05	.053	.027	.354	.239	.027
	.0260	1.190	1.150	.237	.358	3.207	.181	2.150E+05	.049	.023	.375	.223	.028
	.0260	.935	1.011	.224	.336	3.004	.172	1.903E+05	.044	.020	.336	.211	.028
	.0260	.650	.839	.000	.303	2.795	.158	1.678E+05	.040	.016	.294	.189	.029
	.0260	.250	.509	.152	.228	2.233	.126	1.066E+05	.029	.009	.219	.166	.030
	.0260	.080	.136	.099	.149	.917	.057	3.030E+04	.007	.001	.147	.098	.056
	.0354	3.210	1.930	.299	.448	4.303	.214	3.475E+05	.060	.016	.412	.275	.027
	.0354	2.730	1.774	.289	.433	4.091	.209	3.224E+05	.056	.032	.431	.267	.028
	.0354	2.225	1.592	.268	.402	3.960	.197	2.953E+05	.053	.029	.373	.249	.028
	.0354	1.770	1.415	.248	.372	3.504	.186	2.478E+05	.050	.025	.347	.231	.028
	.0354	1.350	1.230	.232	.345	3.654	.177	2.166E+05	.045	.021	.327	.218	.029
	.0354	.970	1.033	.209	.311	3.296	.163	2.035E+05	.040	.017	.297	.195	.029
	.0354	.680	.753	.192	.285	2.979	.153	1.720E+05	.035	.013	.275	.183	.030
	.0354	.500	.731	.175	.262	2.785	.142	1.492E+05	.031	.011	.251	.168	.031
	.0354	.225	.476	.146	.219	2.174	.122	1.003E+05	.022	.006	.213	.142	.035
	.0354	.080	.281	.117	.175	1.601	.101	6.121E+04	.014	.003	.172	.115	.041
	.0440	3.265	1.946	.280	.420	4.633	.204	3.568E+05	.057	.032	.399	.259	.027
	.0440	2.680	1.757	.270	.405	4.337	.199	3.252E+05	.052	.028	.377	.251	.029
	.0440	2.145	1.562	.249	.373	4.182	.187	2.953E+05	.049	.024	.349	.233	.028
	.0440	1.810	1.431	.242	.363	3.943	.183	2.725E+05	.045	.022	.341	.227	.029
	.0440	1.380	1.242	.219	.329	3.761	.170	2.421E+05	.042	.019	.310	.207	.029
	.0440	1.000	1.050	.203	.304	3.443	.160	2.081E+05	.037	.015	.290	.193	.030
	.0440	.745	.897	.184	.276	3.251	.148	1.814E+05	.034	.012	.264	.176	.030
	.0440	.400	.651	.157	.236	2.763	.130	1.355E+05	.026	.008	.227	.151	.032
	.0440	.095	.299	.113	.169	1.762	.098	6.537E+04	.013	.003	.156	.111	.041
	.0440	.030	.168	.090	.135	1.247	.080	3.785E+04	.008	.001	.134	.089	.050
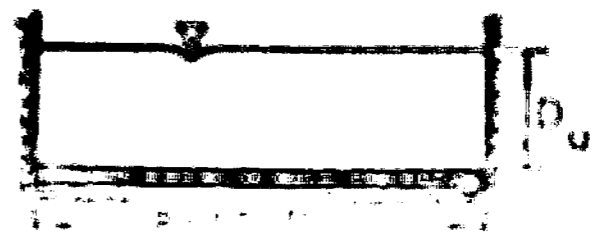
TABLE A·3 SUMMARY OF DATA AND COMPUTATION

KIND OF ROUGHNESS	S_o	ΔH (ft)	Q (ft³/sec)	D_o (ft)	A (ft²)	U (ft/sec)	F_o	N_R	R_w (ft)	A_w (ft²)	A_b (ft²)	R_b (ft)	n_A
1	2	3	4	5	6	7	8	9	10	11	12	13	14
WOODEN SLOPE	.0354	3.190	1.924	.214	.321	5.993	.166	3.769E+05	.099	.042	.273	.186	.015
	.0354	2.669	1.750	.204	.312	5.504	.163	3.450E+05	.090	.037	.275	.143	.014
	.0354	2.285	1.587	.199	.294	5.384	.157	7.194E+05	.056	.034	.265	.177	.015
	.0354	1.860	1.452	.177	.265	5.467	.147	2.958E+05	.074	.031	.235	.157	.015
	.0354	1.190	1.247	.159	.234	5.228	.131	2.501E+05	.051	.026	.213	.142	.015
	.0354	1.040	1.072	.141	.212	5.067	.110	2.272E+05	.077	.022	.190	.135	.01-
	.0354	.870	.976	.130	.195	5.007	.111	2.009E+05	.076	.028	.175	.117	.013
	.0354	.600	.804	.112	.168	4.757	.097	1.762E+05	.071	.016	.152	.101	.013
	.0354	.350	.607	.091	.135	4.447	.081	1.393E+05	.057	.012	.125	.043	.012
	.0354	.150	.398	.064	.096	4.083	.059	9.049E+04	.055	.007	.089	.059	.016
	.0404	3.620	2.055	.218	.327	6.284	.169	4.009E+05	.097	.042	.285	.190	.015
	.0404	2.656	1.746	.199	.299	5.849	.157	3.479E+05	.087	.034	.264	.176	.015
	.0404	2.350	1.640	.189	.284	5.785	.151	3.298E+05	.085	.032	.251	.161	.015
	.0404	1.985	1.493	.178	.267	5.614	.144	3.051E+05	.081	.029	.238	.159	.015
	.0404	1.625	1.351	.160	.240	5.628	.132	2.603E+05	.082	.026	.214	.143	.014
	.0404	1.223	1.170	.146	.213	5.343	.122	2.466E+05	.076	.022	.197	.131	.014
	.0404	1.005	1.050	.132	.198	5.303	.112	2.249E+05	.075	.020	.178	.119	.014
	.0404	.790	.928	.121	.191	5.115	.104	2.013E+05	.071	.017	.164	.110	.013
	.0404	.490	.724	.099	.147	4.922	.087	1.612E+05	.067	.013	.134	.083	.012
	.0404	.260	.520	.075	.113	4.620	.068	1.190E+05	.061	.009	.103	.059	.011
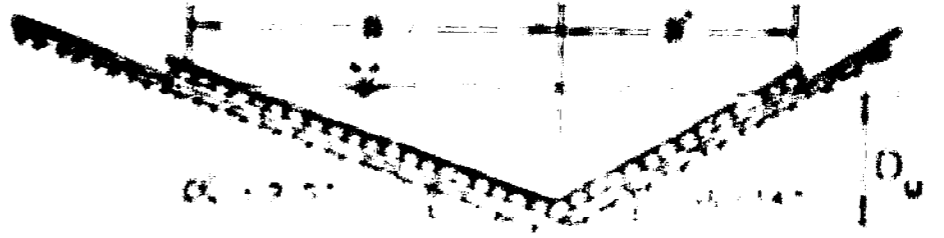
TABLE A·4   SUMMARY OF DATA AND COMPUTATION

KIND OF ROUGHNESS	DATA		COMPUTATION										
	S_o	ΔH ft	Q m³/sec	D_o ft	B ft	D ft	$B+D$ ft	A ft²	U ft/sec	P ft	R_h ft	N_R	$n_{A.T}$
ASTROTURF No.1													
	.0400	4.650	2.930	.416	2.422	1.772	4.243	.936	3.171	4.468	.211	2.490E+05	.037
	.0400	4.450	2.850	.432	2.407	1.746	4.253	.919	3.102	4.431	.209	2.444E+05	.037
	.0400	4.210	2.750	.427	2.368	1.716	4.224	.893	3.204	4.363	.204	2.382E+05	.037
	.0400	3.680	2.600	.414	2.293	1.647	4.076	.444	3.247	4.227	.142	2.352E+05	.036
	.0400	2.910	2.300	.395	2.243	1.615	3.899	.772	2.979	4.036	.191	2.315E+05	.037
	.0400	2.450	2.100	.391	2.222	1.536	3.999	.760	2.762	4.276	.142	2.050E+05	.039
	.0400	1.930	1.600	.353	2.165	1.516	3.672	.635	2.745	3.472	.160	1.845E+05	.038
	.0400	1.440	1.440	.341	2.040	1.419	3.445	.617	2.571	3.635	.171	1.733E+05	.038
	.0400	.500	1.210	.323	1.516	1.373	3.224	.530	2.255	3.343	.158	1.367E+05	.042
	.0400	.170	.550	.206	1.534	1.041	2.619	.348	1.579	2.711	.126	7.662E+04	.053
	.0700	4.860	3.000	.401	2.315	1.630	3.945	.792	3.790	4.087	.194	2.772E+05	.035
	.0700	4.650	2.900	.396	2.289	1.610	3.899	.772	3.757	4.036	.191	2.714E+05	.035
	.0700	4.290	2.850	.365	2.243	1.577	3.820	.741	3.773	3.955	.187	2.674E+05	.034
	.0700	3.780	2.600	.373	2.191	1.541	3.731	.707	3.677	3.863	.183	2.542E+05	.034
	.0700	3.040	2.350	.375	2.165	1.524	3.692	.692	3.333	3.822	.151	2.332E+05	.037
	.0700	2.500	2.100	.367	2.064	1.451	3.515	.627	3.347	3.639	.172	2.140E+05	.036
	.0700	1.935	1.640	.342	1.977	1.390	3.367	.575	3.195	3.486	.165	1.994E+05	.037
	.0700	1.350	1.550	.327	1.390	1.329	3.219	.526	2.945	3.333	.158	1.757E+5	.039
	.0700	.740	1.150	.300	1.734	1.220	2.954	.443	2.535	3.055	.145	1.421E+05	.042
	.0700	.160	.420	.245	1.416	.936	2.412	.295	1.421	2.497	.118	6.353E+04	.067
	.0800	5.910	3.330	.391	2.260	1.589	3.850	.753	4.385	3.995	.189	3.123E+05	.032
	.0800	4.770	2.900	.353	2.214	1.557	3.771	.722	4.016	3.904	.185	2.805E+05	.034
	.0800	4.230	2.800	.374	2.162	1.520	3.682	.689	4.066	3.812	.181	2.774E+05	.033
	.0800	3.750	2.600	.367	2.121	1.492	3.613	.663	3.921	3.741	.177	2.625E+05	.034
	.0800	3.110	2.450	.357	2.064	1.451	3.515	.627	3.935	3.639	.172	2.543E+05	.033
	.0800	2.670	2.150	.353	2.040	1.435	3.475	.613	3.505	3.598	.170	2.257E+05	.037
	.0800	2.070	1.950	.340	1.965	1.382	3.347	.569	3.427	3.466	.164	2.125E+05	.037
	.0800	1.440	1.610	.315	1.821	1.280	3.101	.483	3.296	3.211	.152	1.894E+05	.036
	.0800	.900	1.250	.295	1.705	1.199	2.904	.429	2.918	3.007	.142	1.570E+05	.039
	.0800	.290	.740	.245	1.416	.996	2.412	.295	2.504	2.497	.118	1.119E+05	.040

KIND of	DATA C_D	DATA ΔH (ft)	COMPUTATION m^2/sec	D_y (ft)	B (m)	A (m^2)	U (m/sec)	P (m)	F_N (m)	N_E	D_{A}
ASTROTURF No.1 (F R)											
	.0420	4.910	3.000	.511	2.954	.755	3.975	3.608	.209	3.141E+05	.0??
	.0620	4.650	2.855	.492	2.844	.700	4.074	3.474	.201	3.039E+05	.031
	.0620	4.230	2.750	.487	2.815	.665	4.012	3.439	.199	3.021E+05	.0??
	.0620	3.750	2.603	.478	2.763	.660	3.937	3.375	.196	2.910E+05	.0??
	.0620	3.060	2.353	.469	2.711	.636	3.697	3.315	.192	2.631E+05	.033
	.0620	2.510	2.170	.446	2.574	.575	3.706	3.149	.183	2.555E+05	.032
	.0620	2.050	1.949	.437	2.526	.552	3.515	3.055	.179	2.375E+05	.033
	.0620	1.430	1.550	.408	2.358	.481	3.222	2.851	.167	2.032E+05	.035
	.0620	.840	1.220	.375	2.185	.413	2.954	2.669	.155	1.727E+05	.036
	.0620	.160	.543	.294	1.699	.250	2.162	2.075	.120	9.826E+04	.042
ASTROTURF (A S)											
	.0800	4.850	2.995	.456	2.809	.683	4.380	3.431	.199	3.291E+05	.035
	.0800	4.580	2.880	.472	2.721	.644	4.473	3.333	.193	3.264E+05	.031
	.0800	4.220	2.750	.464	2.682	.622	4.419	3.275	.190	3.171E+05	.031
	.0800	3.580	2.550	.452	2.613	.590	4.319	3.191	.185	3.018E+05	.032
	.0800	3.110	2.360	.441	2.549	.562	4.199	3.114	.181	2.863E+05	.032
	.0800	2.550	2.150	.428	2.474	.529	4.061	3.022	.175	2.697E+05	.032
	.0800	2.070	1.920	.414	2.393	.495	3.876	2.923	.169	2.481E+05	.033
	.0800	1.420	1.630	.388	2.243	.435	3.677	2.740	.159	2.206E+05	.034
	.0800	.530	.980	.334	1.931	.322	3.940	2.358	.137	1.570E+05	.037
	.0800	.230	.640	.294	1.699	.250	2.562	2.075	.120	1.165E+05	.040

REFERENCES

CHOW, V. T., Open Channel Hydraulics, McGraw-Hill Book Company, New York, 1959.

EINSTEIN, H. A., "Method of Calculating the Hydraulic Radius in a Cross Section with Different Roughnesses", Trans., ASCE, Vol. 107, 1942, pp. 575-577.

GRAF, W. H., Hydraulics of Sediment Transport, McGraw-Hill Book Company, New York, 1971.

HORTON, R. E., "Separate Roughness Coefficients for Channel Bottom and Sides", Engineering News Record, Vol. 111, No. 22, November 30, 1933, pp. 652-653.

PARSON, D. A., "Vegetative Control of Stream Bank Erosion", Miscellaneous Publication 970, U. S. Department of Agriculture, 1963, pp. 130-136.

REE, W. O., "Hydraulic Characteristics of Vegetation for Vegetated Waterways", Agr. Eng. 30(4), 1949, pp. 184-187.

REE, W. O. et al., "Flow of Water in Channels Protected by Vegetative Lining", U. S. Conservation Service, Technical Bulletin, No. 967, February 1949.

YEE, P. P., "Hydraulic Performance of Highway Drainage Inlets Used in Pennsylvania", Thesis Presented to the Graduate Committee of Lehigh University in Candidacy for the Degree of Master of Science, 1972, pp. 13-14.

VITA

Chhun V. Heang was born on December 2, 1945 in Kompong Cham, a provincial capital of the Khmer Republic. He is a son of Mr. Leang Chhun Nguon and Mrs. Ros Kim Ly.

In 1952 he started the primary school, "Ecole de Suong", and received the "Certificat d'Etudes Primaire" six years later in 1958. He received the first high school diploma, the "Diplôme d'Etudes Secondaires du Premier Cycle", in 1962 and the second, the "Baccalauréat de la Première Partie", in 1964. He earned the third and final high school diploma, the "Baccalauréat de la Deuxième Partie", in 1965. In late 1965 he began in Phnom Penh his engineering education at the "Institut Technique Superieur de l'Amitié Khméro-Soviétique" in the field of hydraulic engineering. In 1967 he received the "Diplôme des Sciences Générales", and on November 28, 1970, the "Diplôme d'Ingénieur de l'Hydrotechnique".

In September 1971 he was admitted to the Graduate School of Lehigh University at Bethlehem, Pennsylvania as a full-time student on a Fulbright-Hays Scholarship.